Neotectonics in Southern Ryukyu arc by means of paleostress analysis

Bull. Fac. Sci., Univ. Ryukyus, No. 76 : 1 −73 (2003)

Neotectonics in Southern Ryukyu arc by means of paleostress analysis

Makoto Otsubo* and Daigoro Hayashi*

*Department of Physics and Earth Sciences, University of the Ryukyus,
Nishihara, Okinawa, 903-0123, Japan

Abstract

Paleostress estimation is essential in understanding the tectonics of the Southern Ryukyu arc. We have used Multiple inverse method (Yamaji, 2000) and Ginkgo method (Yamaji, 2003) to detect paleostress from the fault-slip data collected in the Southern Ryukyu arc where 23 groups of stress (stresses A-W) are devided. We suggest that stress transition in the Southern Ryukyu arc is more complex than those from the previous studies. As the slickenside of faults in the Ryukyu Group can be measured, detailed stress transition is deduced. Stress field of the after Ryukyu Group in the Southern Ryukyu arc is divided into three zones; Miyako island and Yaeyama islands excluding for Hateruma island (MY zone), Hateruma island (HA zone) and Yonaguni island (YO zone).

We have tried to re-create a complex stress transition after the deposition of the Ryukyu Group by the finite element method imposed on the convergent rate of the Philippine Sea Plate (present, 1 Ma ago and 2 Ma ago). We have re-created stress field in the Southern Ryukyu arc by comparison between the stress pattern detected by the fault-slip analysis and that simulated by the finite element method. From the result of the finite element method, we have proposed that the stress field is caused by the arc-parallel stretching which is responsible to the increasing curvature of the whole arc accompanying the still active back arc basin (Okinawa Trough) proposed by Fabbri and Fournier (1999) and Fabbri (2000). Before 1 Ma when the distance between the Yonaguni island and the collision zone at Taiwan is the nearest by the westward migration of the Philippine Sea Plate, strike-slip fault regime of after Ryukyu Group detected in the Yonaguni island is recognized. This is caused by the effect of collision at Taiwan. Progressive rifting of the Okinawa Trough before 1 Ma gave rise the stress transition of the after Ryukyu Group from NW-SE extension to NE-SW extension in the MY zone. Strike-slip fault regime detected in the Hateruma island is caused by the shear under the influence of oblique subduction because the Hateruma island is located near the Ryukyu Trench. These results give us the useful information to reconstruct the neotectonic evolution in the Southern Ryukyu arc after 1 Ma.

1. Introduction

Southern Ryukyu arc (Fig. 1) is one of the interesting areas to study geology because this area includes various geological components that are oblique subduction of oceanic plate and rifting of back arc basin and collision between continental plate and oceanic plate. Complex geological history is expected in the area. In the Southern Ryukyu arc, a great deal has been investigated about seismic reflection profile, petrology of volcanic rock, gravity anomaly and focal mechanism of earthquake. Many hypotheses have been put forward to explain tectonics around the Southern Ryukyu arc (*e.g.* Lee *et al.*, 1980; Kimura, 1985; Letouzey and Kimura, 1985, 1986; Sibuet *et al.*, 1987; Furukawa *et al.*, 1991; Park *et al.*, 1998; Sibuet *et al.*, 1998; Shinjo *et al.*, 1999; Wang *et al.*, 1999; Kong *et al.*, 2000; Hsu *et al.*, 2001; Kubo *et al.*, 2001). However little has been stated about the transition of paleostress and tectonics. It is not enough to discuss tectonics around this area because

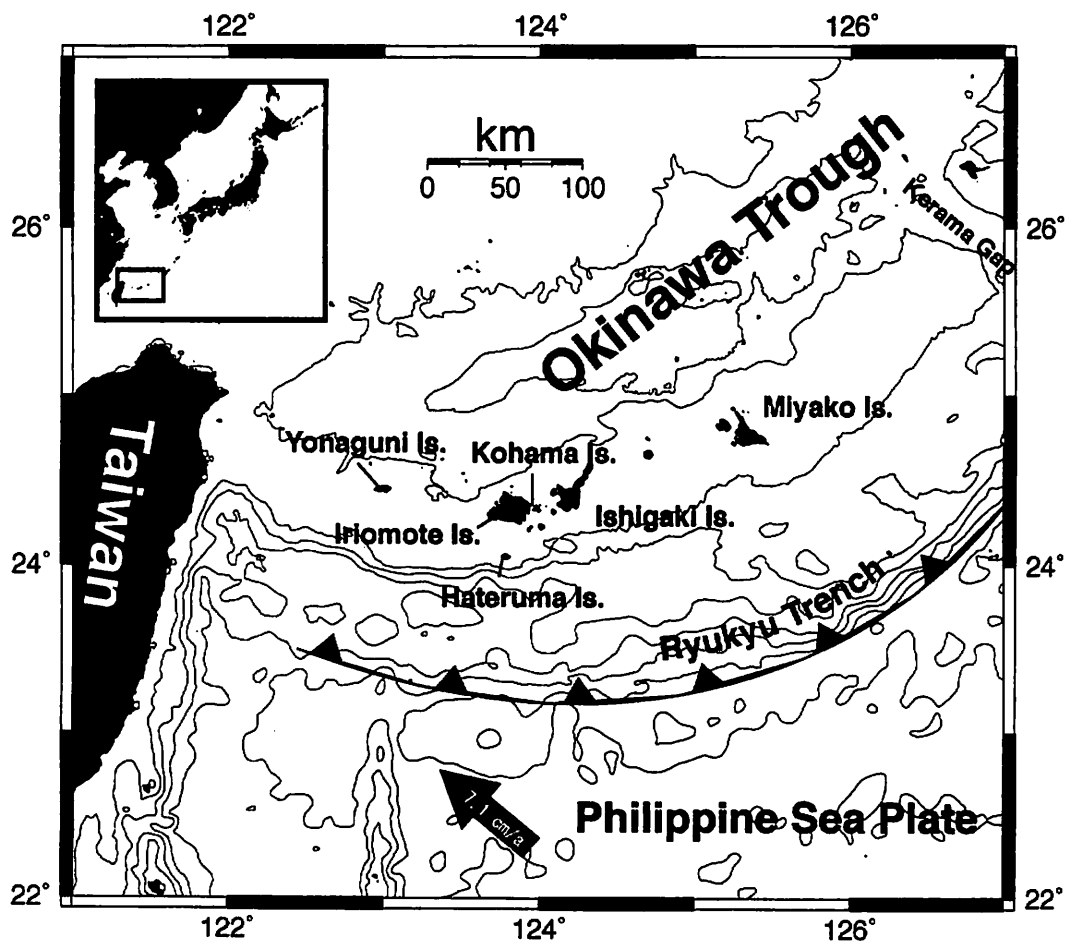

Fig. 1. Tectonic setting of the Southern Ryukyu area. The solid arrow indicates the direction of plate convergence after Seno et al. (1993).

the estimation of tectonic stress is important for structural geologists to contribute to tectonics studies (Pollard, 2000). Therefore, we need to understand paleostress within crust for the construction of tectonics. We have measured the direction of principal stress axes from meso-scale fault by fault analysis. Fault analysis in offshore may be key to construct tectonics around the Southern Ryukyu arc. Kuramoto and Konishi (1989) and Fabbri and Founier (1999) tried to measure paleostress in the Southern Ryukyu arc by the fault analysis. Although new tectonics around the Southern Ryukyu arc were proposed by them, their results are not true because their method has several problems. Although Kuramoto and Konishi (1989) used conjugate fault method to detect plaeostress, the stress direction obtained by the conjugate fault method is correct only in a special case. If all faults are created in one tectonic period and are conjugate faults, plane strain state occurs in the perpendicular plane to σ_2 axis. Many faults are not always conjugated because the strain state is generally three-dimensional. Thus the classic method can not obtain correct stress fields (Yamaji, 2001). Although Fabbri and Founier (1999) used classic inverse method to detect plaeostress, the popular and classic inverse method typified by those of Angelier (1979, 1984, 1990) and Gephart and Forsyth (1984) determines only one stress from a given fault assemblage because classic inversion method (*e.g.* Angelier's method) assume that all faults moved in response to a single stress state (Engelder, 1992). If fault-slip data is heterogeneous, it is a difficult task to separate stresses from the heterogeneous fault-slip data (Yamaji, 2001). Because the Southern Ryukyu arc is a complex tectonic system, more paleostress must be existed in the arc. Therefore, we need to detect pleostress in detail by the new methods.

The aim of this paper is to detect detailed stress from fault-slip data obtained from the field by means of the new methods (Multiple inverse method and Ginkgo method), and to reconstruct tectonic regime by the finite element method.

2. Geology

2.1. Geological setting of the Southern Ryukyu arc

The Ryukyu islands represent an active arc-trench system, which extends Kyushu and Taiwan for a distance of 1200 km. The Ryukyu arc is being subducted by the Philippine Sea Plate along the Ryukyu Trench. Okinawa Trough is in an embryonic stage of back-arc basin spreading. The arc is further divided into three slivers (North, Central and South), which are respectively bounded by Tokara Channel and Miyako Depression (Kerama Gap) (Konishi, 1965). Southern Ryukyu arc is located between Kerama Gap and Taiwan (Fig. 1).

The Southern Ryukyu arc differs from the Central-Northern Ryukyu arc in several ways. For example, pre-Middle Miocene basement rocks outcropping there resemble those of the Inner Zone of Southwest Japan, rather than the Outer zone. In contrast, the Outer zone can be traced down to the Central via the Northern Ryukyu arc (Konishi, 1965; Kizaki, 1978). A chain of Quaternary volcanos (both active and dormant) is distinct in the

Northern and Central Ryukyu arc, whereas only a few monogenetic volcanos are known in the Southern Ryukyu arc. There are differences in the dip angle of the subducting slab, the Philippine Sea Plate, (Carr *et al.*, 1973; Shiono *et al.*, 1980), morphology of the fore arc region, and the evolutionary stage of Okinawa Trough (Sibuet *et al.*, 1987), between the Southern Ryukyu arc and the Central-Northern Ryukyu arc. It is pointed out that the Philippine Sea Plate is obliquely, but not normally, subducting into the Southern Ryukyu arc, where the converging rate is estimated as about 70 km/Ma toward the N55W direction (Seno, 1977).

2.2. Geology of the Southern Ryukyu islands

Fig. 2 shows the stratigraphy of study area. The geology of the Ryukyu arc was synthesized by Konishi (1965) and Kizaki (1978, 1985, 1986). The Southern Ryukyu islands are composed of pre-Tertiary accretionary complex (Tomuru Formation and Fusaki Formation), Eocene green tuff (Nosoko Formation) and platform limestone (Miyaragawa

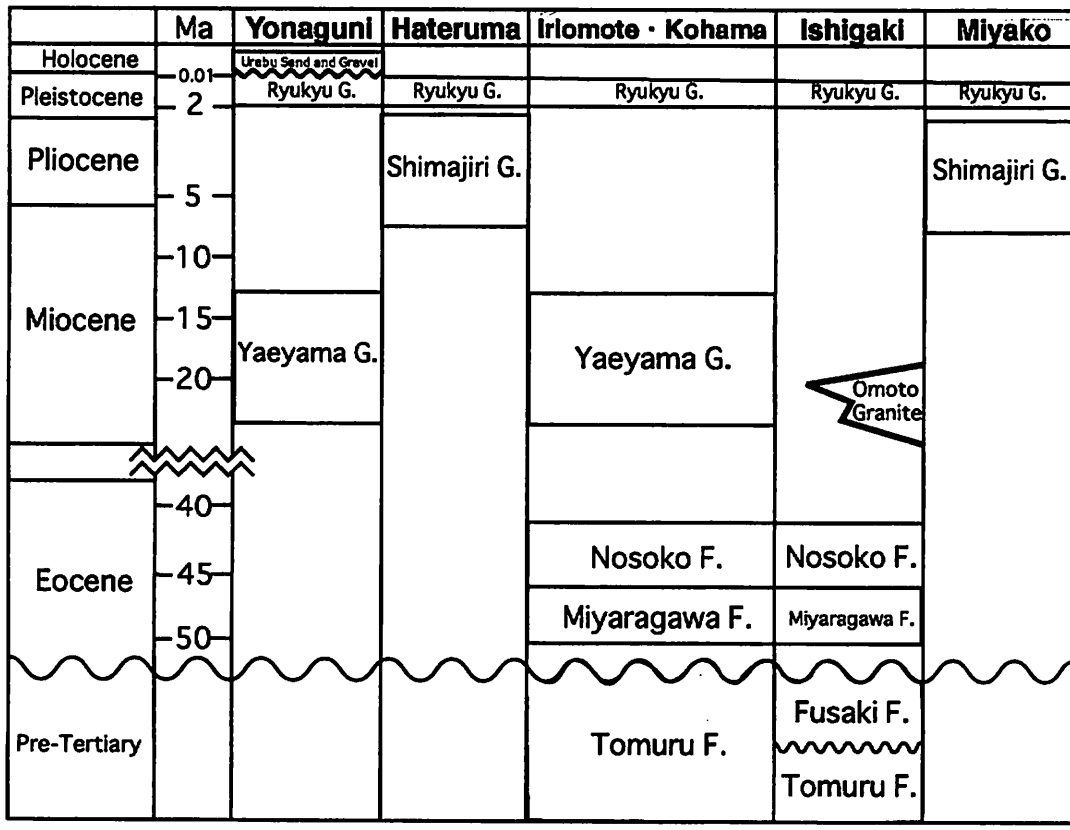

Fig. 2. Stratigraphy of the Southern Ryukyu islands (compiled from Ujiie and Oki (1974), Sakai et al. (1978) and Kizaki (1985, 1986)).

Formation), early to middle Miocene alternate bed of sandstone and mudstone (Yaeyama Group), Pliocene mudstone and siltstone (Shimajiri Group), Pleistocene mainly Ryukyu limestone (Ryukyu Group) and Holocene deposits. We have researched to detect paleostress by fault-slip analysis in the Miyako island, Ishigaki island, Kohama island, Iriomote island, Hateruma island and Yonaguni island.

2.2.1. Miyako island

Miyako island is the northernmost island of the Southern Ryukyu arc, and lies about 250 km southwest from Naha in Okinawa island and about 100 km northeast from the Ishigaki island (Fig. 1). The whole section (2.2.1) hereafter is quoted from the article (Otsubo and Hayashi, 2001; Kizaki, 1985).

Miyako island shows a flat triangle with two equal sides. The length of NW-SE side is about 30 km. Shimajiri Group is the basement of the island, which consists of Miocene to lower Pleistocene formation, and is unconformably covered by the Ryukyu Group. Several faults run along NW-SE and NNW-SSE in the island (The Research Group for Active Faults of Japan, 1991). Southwestern coast shows a steep scarp composed of the Ryukyu Group with a few meters to about 40 m in height.

Base of the Shimajiri Group is exposed along the scarps of the eastern side of the island. It is difficult to observe the outcrop of the Group in the southern side because of its steep scarps. The Shimajiri Group consists of mudstone and sandy mudstone, and shows soft to semiconsolidated state in one of the weathered outcrops. Outcrops show generally weathering in its upper part. Thick formation at several outcrops contain clay. In the alternation of sandy mudstone and mudstone, some sandy mudstone beds protruded by differential erosion. The Shimajiri Group shows the anticline whose fold axis directs to NE-SW and plunges to SW having is 4 to 6 km wavelength.

The Ryukyu Group (Ryukyu Limestone) covers extensively the island and its lithostratigraphic column is observed in the steep scarps of the southern coasts. The Group consists of basal conglomerate, coral limestone, rudstone and floatstone from lower to upper, which shows transgressive facies from coarse (deep) to fine (shallow). The Group shows anticline whose fold axis directs to NW-SE and which passes through the center of the island. Both limbs of the anticline dip 10 degrees. There are many faults whose offset is less than 30 m and whose strike is parallel to fold axes, and they show stair step shape. The anticline forms a low ridge hill of the island. The undulation of surface reflects the undulation of the basement of the island. Cuesta is characteristic to the Miyako island and is derived from the fault topography (Otsubo and Hayashi, 2001).

2.2.2. Ishigaki island

Ishigaki island is an easternmost island of the Yaeyama islands, which lies about 350 km west-southwest from Naha in Okinawa island and about 200 km east from northeastern

edge of Taiwan (Fig. 1). Yaeyama metamorphic rocks are the basement of the island, which are divided into Tomuru Formation and Fusaki Formation in terms of their metamorphic phase and degree, and structure. The Yaeyama metamorphic rocks are unconformably covered with Miyaragawa Formation (platform-type limestone), Nosoko Formation (pyroclastic rocks and green tuffs) and Quaternary gravels and limestones (Kizaki, 1985). The Miocene intrusive granite, Omoto Granite, is also existed in the island. There are no clear major faults in the island (The Research Group for Active Faults of Japan, 1991). The whole section (2.2.2) hereafter is quoted from the article (Kizaki, 1986).

The oldest rocks of the islands may be represented by the Tomuru Formation of the Yaeyama metamorphic rocks of Southern Ryukyu arc, which are composed of greenschist, blueschist, silious schist, pelitic schist, metagabbro of the glaucophane schist facies and also pillow lavas and hyaloclastic rocks in less metamorphosed areas. The metamorphic Tomuru Formation is shown to be distributed only throughout the Yaeyama islands but also in the area of the Miyako islands because the glaucophane schist-bearing conglomerate occurs in the basal part of the Shimajiri Group of Pliocene age in the islands.

The radiometric ages of the metamorphism have been dated as Jurassic: 159-175 Ma by the K-Ar method (Shibata *et al.*, 1968; Nishimura *et al.*, 1983) and 195 Ma by the Rb-Sr method (Shibata *et al.*, 1972). According to the frequency diagram of the radiometric ages of the high-pressure metamorphic rocks from southwest Japan and Taiwan (Nishimura, 1893), the age of the Yaeyama metamorphic rocks is to be correlated with the older episode of the Nagasaki metamorphic rocks and with the younger episode of the Sangun metamorphic rocks in the Inner Belt of southwest Japan. It is therefore suggested that the Yaeyama metamorphic rocks could be attributed to the high-pressure metamorphic rocks of the Inner Belt of southwest Japan and also the original rocks could be Triassic to Paleozoic, similar to other high-pressure metamorphic rocks in southwest Japan and Taiwan (Yen, T.P, 1971).

Structural analysis has revealed two main deformation phases; first phase folding, with a NW-SE axis, is principal and associated with a high pressure metamorphism having preferred mineral lineation parallel to the fold axis, and the second phase, of close to open minor folds with E-W axis, superimposes on the first phase folding to result in dome and basin structures in some places (Fujii and Kizaki, 1983).

The Fusaki Formation of the Yaeyama metamorphic rocks, composed of phyllite, sandstone, chert and conglomerate without greenstone, has been regarded as a lower grade chlorite-sericite phyllite of the metamorphics of the same age. However, the Formation, together with the Eocene Nosoko Formation, is over thrust by the Tomuru Formation and it is not deformed by the NW-SE trending folds of the first phase but only by the E-W trending, open and gentle folds of the second phase. A chert bed of the Formation produces radioralia older than lower Cretaceous. So, the Fusaki Formation may have been deposited between the Jurassic and lower Cretaceous, after the metamorphism of the Tomuru

Formation. The Fusaki Formation is distributed in the southern part of Ishigaki island and to the north of Miyako island where 38 Ma phyllite (K-Ar method) has been obtained from a bores core (Aiba and Sekiya, 1979). However, such an Eocene metamorphism is not known in North-Central Ryukyu and further north, so that the rock probably belongs to the Fusaki Formation.

The Miyaragawa and Nosoko Formations of Eocene age occur only in the Yaeyama islands of Southern Ryukyu, in addition to the Eocene formation of the Shimanto Supergroup of North-Central Ryukyu. The Miyaragawa Formation, composed of limestones and sandstones, contains various foraminifera such as Nummulites, Discocyclina, Pellatispira. Some of these fossils are also found in the tuffs and tuffaceous sandstones of the Nosoko Formation which is composed of pyroclastic rocks and andesite lavas.

The Miyaragawa Formation represents a littoral facies whereas the Eocene flysch sediments occur in the Shimanto supergroup, and further deformation and meta- morphism are not recognized in the Miyaragawa and Nosoko Formation but do clearly in the Supergroup of North-Central Ryukyu. The paleomagnetic investigation of the Nosoko Formation revealed that a clockwise rotation of 40° took place after the deposition of the Formation, probably in the Oligocene (Sasajima, 1977).

The Eocene volcanism was only developed in Southern Ryukyu whereas the Miocene "Green Tuff Volcanics" are distributed throughout North-Central Ryukyu from Kyushu; nevertheless the rock facies are quite similar to each other. However, the pyroxene andesites of the Southern Ryukyu indicate a lower alkali-lime index (58.3) than the Miocene andesites (61.8) of North-Central Ryukyu (Matsumoto, 1964).

Ryukyu Group exposed in Ishigaki Group is called Ohama Formation. The formation is mainly divided in Ryukyu limestone and Sand and gravel bed (Kizaki, 1985).

2.2.3. Kohama island

Kohama island is a small island which lies about 15 km west from the Ishigaki island and about 3 km east from the Iriomote island (Fig. 1). However, the Kohama island is the important island to study stratigraphic relationship of strata in Yaeyama area because all of the strata distributed in the Yaeyama islands are existed in the island. The whole section (2.2.3) hereafter is quoted from the article (Kizaki, 1985).

Hunazaki metamorphic rock is the basement of the island, which is compared with Tomuru Formation, and is unconformably covered by Koki limestone, Komasaki Formation (pyroclastic rock), Birumazaki Formation (alternate bed of sandstone and mudstone) and Quaternary gravels and limestones. No clear major fault is existed in the island.

Koki limestone, Komasaki Formation and Birumazaki Formation are correspond to Miyaragawa Formation, Nosoko Formation and Yaeyama Group, respectively. Quaternary gravels and limestones are composed of terrace conglomerate and Ururo limestone (Kizaki, 1985).

2.2.4. Iriomote island

Iriomote island is the fifth large island which lies about 20 km west from Ishigaki island and about 180 km east from northeastern edge in Taiwan (Fig. 1). The whole section (2.2.3) hereafter is quoted from the article (Kizaki, 1985).

In Iriomote island, metamorphic rock Tomuru Formation is the basement and is unconformably covered by Miyaragawa Formation, Nosoko Formation and Iriomote Formation (Yaeyama Group), Sonai Conglomerate and Sumiyoshi Formation (Ryukyu Group) (Quaternary gravel and limestone). Iriomote Formation is widely exposed in Iriomote island. No clear major fault (lineament) is existed in the island (The Research Group for Active Faults of Japan, 1991).

Tomuru Formation in the island consists of basic schist, muddy schist, quartzitic schist and metamorphic gabbro. The bed trends northeast to north and dips northwestward. Miyagawa Formation is the platform type limestone which is exposed in a limited area at the upper reaches in Yonara river. The formation lies horizontally whose thickness is about 20 m. Nosoko Formation is divided into two parts. Lower part of the formation mainly consists of andesitic volcanic breccia, andesitic tuff breccia and andesitic lava, while the upper part consists of dacitic lava, rhyolitic tuff, rhyolitic breccia tuff and rhyolitic lava. Dacitic dyke is also exposed in the formation. The thickness of the formation is about 300 m. Pre-Miocene formations, Tomuru, Miyaragawa and Nosoko Formation are exposed in a limited area in the northeastern part of region.

Iriomote Formation is composed of conglomerate, sandstone and siltstone, coal bed, and calcareous sandstone, which covers unconformably the Nosoko Formation. The thickness is about 700 m. The bed trends northeast and dips westward. The formation is lithologically divided into A, B, C, D, E, F and G beds. In particular, the bed F is called Utibanare coal-bearing member. Sonai Conglomerate is composed of sandstone, calcareous sandstone and shell limestone whose gravels are pebbles or flat gravel in 6 cm diameter. All the Sonai Conglomerates and derived from the Iriomote Formation. However the age of the formation remains unknown. Conglomerate, sandstone and limestone included in Ryukyu Group are called Sumiyoshi Formation. The bed is found in a scattered pattern along the coast in the island. The bed is considered the upper part of the in Ryukyu Group (Kizaki, 1985).

2.2.5. Hateruma island

Hateruma island is a small island and the southernmost island of the Ryukyu islands, which lies about 20 km south from the Iriomote island (Fig. 1). The whole section (2.2.5) hereafter is quoted from the article (Kizaki, 1985).

Although geological character in the island looks like that of the Kikai island, southern part in the Okinawa island and Miyako island, pre-Quaternary basement rock (Shimajiri Group) shown in other islands (*e.g.* Miyako island) have not been exposed in the island.

Therefore, most of the formations in the island are belong to the Ryukyu Group. Several major faults run along NW-SE and WNW-ESE in the island, which may be strike-slip faults (The Research Group for Active Faults of Japan, 1991).

Basement of the island is dark bluish gray mudstone observed in a limited area. The formation is correlated with the Shimajiri Group by the lithofacies, color, degree of consolidation and the relationship to the Ryukyu Group. Ryukyu Group is mainly composed of limestone and exposured widely in the island. The Group have formed three step terrace, and the Group is divided into three formations Huka Formation, Hateruma Formation and Takanazaki Formation by Nakamori (1986). Yamada and Matsuda (2001) have divided the Group into four units. The unit 1 is only accumulative or backed develop type and unit 2, 3 and 4 are advance develop type (Kizaki, 1985).

2.2.6. Yonaguni island

Yonaguni island is the hexagonal-shape island and westernmost island of the Ryukyu islands which lies about 170 km east from the northeastern edge of Taiwan (Fig. 1). The whole section (2.2.6) hereafter is quoted from the article (Kizaki, 1985).

Yaeyama Group, which is composed of alternate bed of sandstone and mudstone is the basement of the island and is unconformably covered by mainly Ryukyu Group (limestone) and Quaternary deposits. Several faults run along NW-SE, NE-SW and E-W in the island. Shape of the island is defined by these faults. Kizaki (1985) reported that three fault systems (NW-SE, NE-SW and E-W) are composed of steeply normal faults.

In Yaeyama Group, the cycle of alternation of the group varies in degree. Most of the Yaeyama sandstones are feldspathic wackes, white bivalves, including oyster, and terrestrial plants are common in the Yaeyama Group throughout the island. Some sedimentary structures such as channel and turbidite sequences are observed. Paleocurrent directions are approximately from north to south (Kuramoto and Konishi, 1989). The thickness of the formation is approximately estimated to be over 1000 m. The formation shows that same unit is observed several times because the bed is cut by normal fault. The bed strikes to northwest and dips southeastward.

Ryukyu Group which overlaps unconformably the Yaeyama Group is divided into the lower Donan Formation and the upper Ryukyu limestone. The Donan Formation is divided into two facies; sand and pebble and boulder. The former is mainly composed of very very fine to fine sand and flat pebbles of feldspathic wacke which is derived from the Yaeyama Group. The thickness of the formation is less than 20 m. Two facies are recognized in the upper Ryukyu limestone; detrital and coralliferous. The thickness of the formation attains 40 m in maximum, and it varies markedly with the local variation of the basement relief. The lowest terrace formed of the coralliferous facies lies at 5-6 m above the present mean tide level along the northern coast. The terrace is dated to be the Last Interglacial (about 0.125 Ma), by ^{230}Th coral age.

Quaternary deposits are divided into the Urabu sand and gravel and the raised reef limestone. In particular, sedimentation of the Urabu sand and gravel relates to the fault formation and tilting movement of the island because the bed is exposed along the major fault system and the thickness increases from north to south within the basin (Kizaki, 1985).

2.3. Paleomagnetic data in the Southern Ryukyu arc

Paleomagnetic investigations have revealed a post-Eocene clockwise rotation of Ishigaki, Iriomote and Miyako islands (Miki *et al.*, 1990; Miki, 1995). Clockwise deflections of paleodeclinations are estimated between 19° (Miki *et al.*, 1990) and 25° (most plausible value (Miki, 1995)). The 25° rotation occurred from 10 Ma ago (age of the youngest rotated rocks) to 6 Ma ago (approximate age of the oldest unaffected rocks) and was not accompanied by the significant N-S translation (Miki, 1995). The absence of any pronounced bathymetric discontinuity between the islands allows us to consider that the Southern Ryukyu arc has been a rigid block since Neogene and rotated as a whole.

3. Methodology

Neotectonics of the Southern Ryukyu arc is deduced by the following process in this paper. Firstly detailed paleostress in the Southern Ryukyu arc is obtained by the fault-slip analysis (Multiple inverse method and Ginkgo method). We have measured fault-slip data (strike and dip of fault plane and trend and plunge of slickenside on fault plane) to detect paleostress. Then, the stress transition of the Southern Ryukyu arc is deduced. Secondarily simulation with the finite element method is performed to find how the stress which detected by the fault-sip analysis is given by the Ryukyu arc and Trench. We take notice of stress pattern (direction and stress state, *e.g.* compression or extension) of the horizontal stress of the Miyako island, Yaeyama islands and Yonaguni island. Finally neotectonics of the Southern Ryukyu arc are deduced by comparison between the stress detected by fault-slip analysis and the stress obtained from finite element method.

4. Fault-slip analysis

Meso-scale fault means the fault which can be observed in the scale of outcrop (Angelier, 1994). Meso-scale faults are frequently observed than the macro-scale faults, and whose amount and sense of displacement are measured easily. Their orders of age are deduced from cross-cut relationship. Meso-scale faults of this kind are used to measure the direction of principal stress axes. Relation of the regional stress field and geometric structure are discussed by the principal stress. If the detected principal stress axes show systematic trend, we consider to obtain the regional stress field which explains the tectonics around there. We measure strike and dip of fault plane, and trend and plunge of slickenside to analyze. These data are called fault-slip data. Multiple inverse method and Ginkgo

method are used to obtain paleostress.

4.1. Fault-slip data in Southern Ryukyu arc

Table 1, 2, 3, 4, 5 and 6 show fault-slip data in the Southern Ryukyu arc which we have measured in the Miyako island, Ishigaki island, Kohama island, Iriomote island,

Table 1. Mesoscale faults data measured in the Miyako island. In slickenline data, data are described by trend and plunge. Sense data indicate fault type. N: normal fault, R: reverse fault, D: dextral strike-slip fault, and S: sinistral strike-slip fault.

Site	Unit	Fault plane	Slickenline	Sense
MR1		N76W60N	N69E45	N
		N10W70E	S44E48	S
		NS70W	S24W48	S
		N84E64S	S13E64	N
		N80W80S	S56W76	N
MR2		N56E60S	S40W46	D
		N20W82E	N18E77	S
MR3		N50E70N	N72E46	S
		N10E66W	S35W43	S
		N20W70E	S58E59	D
		N4E66E	S89E66	N
		N10E80N	S59W74	N
		N64W22S	S40W21	N
		N84W50N	N37E46	N
		N42E72N	N32W71	N
		N40W72N	N19E69	N
		N44W62S	S32W61	N
		N70W72N	N20E72	N
		N30E50S	S76E49	N
	Ryukyu Group	N32W80W	N90W78	N
MR4		N34W78S	N89W75	N
		N26W76W	S81W75	N
		N44W70S	S37W70	N
		N44W80W	S46W80	N
		N30W80W	S38W79	N
		N46W80N	N27W62	D
		N40W72W	S76W70	N
		N26W76W	S36W74	N
		N48W80S	S69W79	N
		N22W72E	N34E69	N
		N20W80E	N38E79	N
		N40W82N	N23E81	N
		N50W78W	S81W74	N
		N44W80N	N28W58	S
		N40W80S	S7W76	N
		N74W68W	S55W62	N
		N46W76W	N72W60	D
		N58W66S	S29E47	S
		N20W80N	N19E74	S

Table 1. continued.

Site	Unit	Fault plane	Slickenline	Sense
MR5	Ryukyu Group	NS72W	N13W35	D
		N10W80W	N42W72	D
		N20W78W	N28W33	D
		N20W76W	N31W37	D
		N10W82W	N26W63	D
MR6		N14W54W	S34W46	N
		N30W68E	S63E53	D
		N10E40E	N90E40	N
MS1	Shimajiri Group	N72E82S	S18E82	N
		N74E82S	S9E82	N
		N80E80S	S29W77	N
		N82E78S	S27E77	N
		N82W80S	S84W54	D
		N86W76S	S68W61	D
		N26E50E	S64E50	N
MS2		N42E46N	N54W45	N
		N40E48N	N38W47	N
		N44E70E	S49E70	N
		N38E46N	N42W46	N
		N52E52N	N28W52	N
		N42E58S	S64E57	N
		N50E60N	N69W57	N
		N46E62N	N49W62	N
		N66E81S	S30E81	N
MS3		N70E68S	S25W60	N
		N70E72S	S8W70	N
		N60E80S	S36W67	D
		N34E80E	S11W66	D
MS4		N80E82S	S62W66	D
		N40E88E	S77E88	N
MS5		N56E84S	S25E84	N
		N30E62N	N55W62	N
		N40E86S	S50E86	N
MS6		N62E74S	S25E74	N
		N54E60N	N49W59	N
MS7		N16E88E	S2W82	D
		N54E80N	S61W33	S
		N50E80N	S74W67	S
		N10W40W	S60W38	N

Table 2. Mesoscale faults data measured in the Ishigaki island. Data format is the same as Table 1.

Site	Unit	Fault plane	Slickenline	Sense
IsR1	Ryukyu Group	N12E84E	N84E84	N
		N4W86W	S84W86	N
		N24W78W	S42W74	N
		N30E78E	S41E77	N
IsR2		N52E88N	N58W88	N
		N80W72N	N7E72	R
IsR3		N54E84E	S40W67	D
		N76E82N	N14W82	N
		N70E66S	S20E66	N
IsR4		N52W80N	S76E18	D
		N42E58S	S48E58	N
IsR5		N60E60W	N30W60	N
IsN1	Nosoko Formation	N70E80S	S20E80	R
		N40E24S	N69E12	S
		N70E90	N70E45	S
		N80E80S	S1W80	R
		N64E88S	S26E88	N
		N80E62S	S10E62	N
		N70E80S	S26E80	N
		N90E80S	S0E80	N
		N62E82N	N30W81	S
		N60E60N	N26E44	N
		N68W68N	N31W56	S
		N50W70S	S61W69	N
		N72W88S	S9W88	N
		N40W42N	N49E42	N
		N24W72N	S29E16	S
		N50E70N	N14E58	D
		N68W78N	N57W43	S
		N30W70S	S27W66	N
		N60W42N	N2W37	N
		N70W70S	S11W70	N
		N30E80N	N60W80	N
		N18W70W	S13W55	D
		N50E70S	S14E68	N
		EW52S	S78E15	S
		N70W60S	S12E56	N
		N80W50S	S0E50	R
		N84W54S	N57E41	R
		N70E80S	S31E80	N

Table 2. continued.

Site	Unit	Fault plane	Slickenline	Sense
IsN2		N30W88E	N60E88	N
		N84E75S	S24E71	N
		N31W51E	N18E43E	N
		N4W88E	N86E88	N
		N80E60S	S52W39	D
		N58E68E	S32E68	N
		N7E69E	N85E69	N
		N50E64S	S50E63	N
IsN3		N40W60N	N33W12	S
	Nosoko Formation	N8E56S	S21E36	D
		N30E80N	N26E24	D
		N30E80N	N26E24	D
		N30W42N	N33E39	N
		N80W72N	N71W27	S
		N70W80S	S64E30	D
		N40W30S	S10E16	N
		N20W70S	S16W57	D
		N20W26S	N40W9	S
		N74E53S	S40W36	S

Table 3. Mesoscale faults data measured in the Kohama island. Data format is the same as Table 1.

Site	Unit	Fault plane	Slickenline	Sense
KR1		N52W82E	N52E82	N
KR2		N80W80S	S37W80	N
		N46W86S	S60W86	N
	Ryukyu Group	N18W80W	S34W79	S
		N64W82N	N40E82	N
		N50W82N	N54E82	N
		N50W82N	N54E82	N
KY1		N52W76N	N38E76	N
		N66W60S	S14W59	N
		EW30S	S26W27	N
	Yaeyama Group	N12E88E	N22E88	N
		NS82E	N83E82	N
		N50W90	N50W90	S
KN1		N26W72E	N38E70	N
		N30E60E	S30E56	N
		N70W80S	S37W80	N
		N40E60E	S21E57	N
		N22W52W	N89W50	N
	Nosoko Formation	N22E88W	S22W10	S
		N30E82W	S33W20	S
		N8E80E	N52E76	N
		N46W70N	S56E25	D
		N30E90	N30E0	S
KN2		EW80S	S17E80	N

Table 4. Mesoscale faults data measured in the Iriomote island. Data format is the same as Table 1.

Site	Unit	Fault plane	Slickenline	Sense
IrY1		N14W52W	S62W51	N
IrY2		N10W78E	N71E78	N
		N36E86E	S40E86	N
		N70E80S	S20W80	N
		N60E80N	N36W80	S
		N20W70E	S84E68	N
		N30W86W	S23W85	N
		N46E76E	S52E76	N
IrY3		N44W66N	N38E66	R
		N22E72S	S86E71	N
		N4W80W	N72W79	N
		N12W72E	S77E70	N
		N74W64S	S84W37	D
		N78W74S	S12W74	N
		N80E20N	N6E19	R
		N10W70E	S72E68	N
		N20W80E	N12W52	S
		N8E70E	S8E37	N
IrY4		N72E60N	N80W39	S
		N28W78W	S70W78	N
		N82E20N	N4E19	N
IrY5		E-W74N	N20E83	N
		E-W70S	S20W79	N
		N70W70S	S9W70	N
IrY6		N74W74W	S27W74	N
	Yaeyama Group	N80W72S	S10W72	N
		N64W74S	S26W74	N
		N50E80S	S89E75	N
		N82E80S	S28W78	N
		N2E82W	N18W69	S
		N2E72W	S59W69	N
		N-S56E	N52E50	N
		N12E78E	S4W34	D
		N84E60S	S18E60	N
		N20W60W	S4W65	D
		N14E52W	S21W48	S
IrY7		N-S70E	S80E68	N
		S10W80E	S7W20	D
		N20W88E	N13W72	S
		N86W76S	S36E72	N
		N40E76S	N66E60	S
		N10E64S	S55E62	N
		N10W86E	S19E64	D
		E-W76S	S63E60	R
		N44E56E	S14E52	N
		N50E70S	S62E68	D
IrY8		N40W82E	N46E39	N
		N30W60E	N48E59	N
		N32W84E	N28W32	S
IrY9		N4W76S	S41W72	N
		N80E78N	N30W77	N

Hateruma island and Yonaguni island. Although previous researchers could not measure the fault-slip data within the Ryukyu Group (Kuramoto and Konishi, 1989; Fabbri and Founier, 1999), we have succeeded to measure them. Fig. 3a shows a photograph of striations on a slickenside of a fault in the Ryukyu Group in the Miyako island. This slickenside looks like a similar slickenside in other units (*e.g.* Nosoko Formation in Ishigaki island (Fig. 3b)).

Table 5. Mesoscale faults data measured in the Hateruma island. Data format is the same as Table 1.

Site	Unit	Fault plane	Slickenline	Sense
HR1	Ryukyu Group	N6W28E	N55E25	R
		N18E80E	N59E75	S
		N18E82W	N72W82	N
HR2		N24W58W	N65W46	S
		N64W84N	N28W80	S
		N52W72E	N87E63	N
		N50W64W	S3E56	R
HR3		N88W70N	N16W69	R
HR4		N76E80S	S61W55	D
HR5		N8W78N	N33E72	D
HR6		N32W62N	N5W40	S
		N82E82S	S68W60	D
HR7		N90E66S	S78W25	D
		N10E68E	N25E33	S
		N26E86N	N24W32	N
		N86W55S	S55W42	N
		N86W66S	S65W47	R

Table 6. Mesoscale faults data measured in the Yonaguni island. Data format is the same as Table 1.

Site	Unit	Fault plane	Slickenline	Sense
YH1	Urabu sand and gravel	N36E63N	N73W62	N
		N4E78W	S89W78	N
		N10E66W	N48W62	N
YH2		N50E86S	S40E86	N
YR1	Ryukyu Group	N4E60E	N62E58	R
		N24W74E	N25E69	R
YR2		N42W80W	S42W80	N
		N10W68W	N54W60	D
		N8W34E	S35E17	D
		N12E56E	N30E24	S
YR3		N40W30E	S85E22	N
		N26W44W	S40W41	N
		N74W74N	N55E70	N
		N52W62N	N38E62	N
		N12W44W	S40W37	R
		N62W42S	S52W39	R
YR4		N88E70S	S26E68	D
YR5		N80E66N	N22E62	N
		N30W80W	S24E78	D
		N42E82E	N80E78	S
YR6		N74E72N	N3W72	N
YR7		N74W42S	S43W39	N
		N30W50E	N19E42	N
YR8		N58W62W	S41W62	N
YR9		N70W80N	N12W78	N
		N28W56W	S48W55	N
YY1	Yaeyama Group	N24E84N	N36W82	N
YY2		N11E77W	N75W77	R
YY3		N80E78S	S10E78	N
		N78W86S	S29W85	N
		N78E86S	S12E86	N
		EW80S	S83E36	D
YY4		N20W76E	S82E74	N
		N26W74E	N28E70	N
		N2E84E	N47E81	S
		N32E82S	N70E77	S
		N74E64N	S10W62	N
YY5		N84E88S	S6E88	N
		N86E85N	N36W85	R
		N29E83E	S45E83	S
		NS78E	N49E74	N
		N76E74N	N22E70	N
		N14W79E	N76E79	N
		N4W82E	S61E81	N

Table 6. continued.

Site	Unit	Fault plane	Slickenline	Sense
YY6		NS87W	S72W87	R
		N8E70W	N85W70	R
YY7		N62E70W	N31W70	N
YY8		N88E66N	N13W66	N
		N88E78N	N7W78	N
YY9		N58E80N	N38W80	N
		N50E70N	N46W70	N
YY10		N60E72N	N23W72	N
		N72E72S	S11E72	N
YY11		N78E78N	N27W78	N
YY12		N49E79N	N51W79	N
YY13		N24W54W	S86W52	N
		N62E86N	N28W86	N
YY14		N16E78W	N30W74	N
		N15E70W	N31W63	N
		N24E72W	N30W68	N
		N28E72W	N28W69	N
		N58W84N	N14E84	N
		N43W83W	S55W83	N
		N69E85W	N32W85	S
YY15		N70E70N	N9E67	N
		N74E64N	N46W61	N
		N52E60N	N85W50	N
	Yaeyama Group	N54E88S	S36E88	R
		N70E64N	N55W59	N
		N74E70N	N58W64	N
		N14E80W	N33W76	R
		N80E80N	N53W78	N
YY16		N74W84N	S88E66	D
		N79W83E	N27E83	N
		N12W84E	N28E81	N
		N16W83E	N74E83	N
		N46W34S	S20W32	N
		N79E73N	N14W73	N
		N8E87W	N64E86	R
YY17		N10E56E	S74E56	R
YY18		N10W80W	N68W78	N
YY19		N56E85N	N34W85	N
		N70E88S	S20E88	S
		N70E86S	S20E86	N
		N56E56N	N36W56	N
		N74E78N	N25W78	N
		N67E67N	N31W67	N
		N70E70N	N11W70	N
		N69E66N	N23W66	N
		N72E72N	N21W72	N

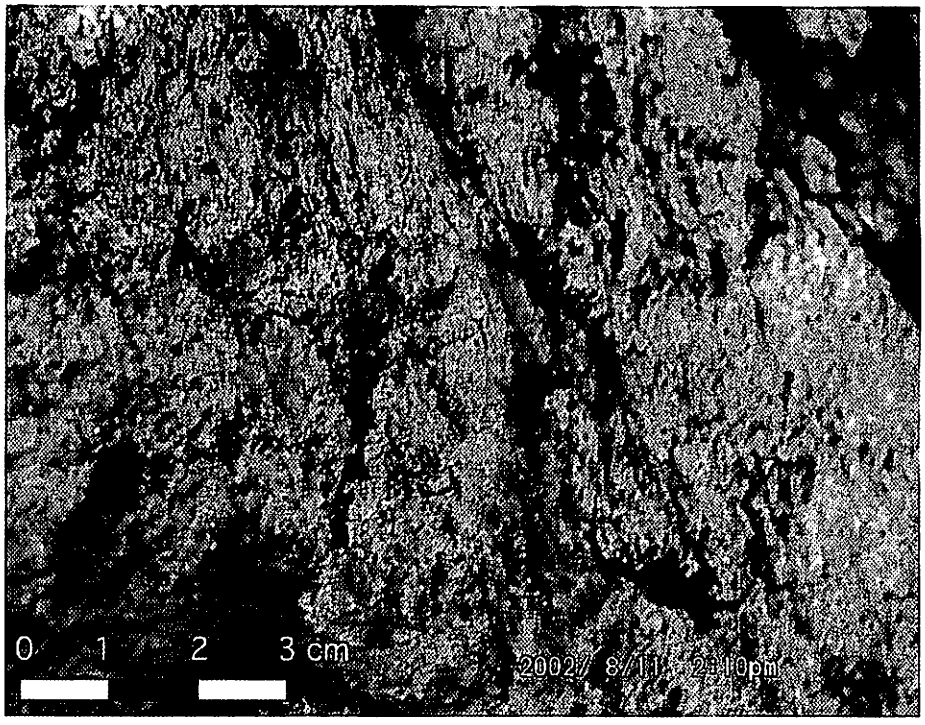

Fig. 3. Photographs of fault slickenside. (a) Slickenside observed within the Ryukyu Group (limestone), in Miyako island. (b) Slickenside observed whitin the Nosoko Formation, in Ishigaki island.

4.1.1. Miyako island

Fig. 4 shows the fault-slip data and the site map measured in the Miyako island. Fault-slip data are shown in lower-hemisphere of equal-area projection. Strike and dip of fault and trend and plunge of slickenside are described in equal-area projection. Sense of the meso-scale fault is shown by two colors; blue and red. Blue means normal fault, while red means reverse fault.

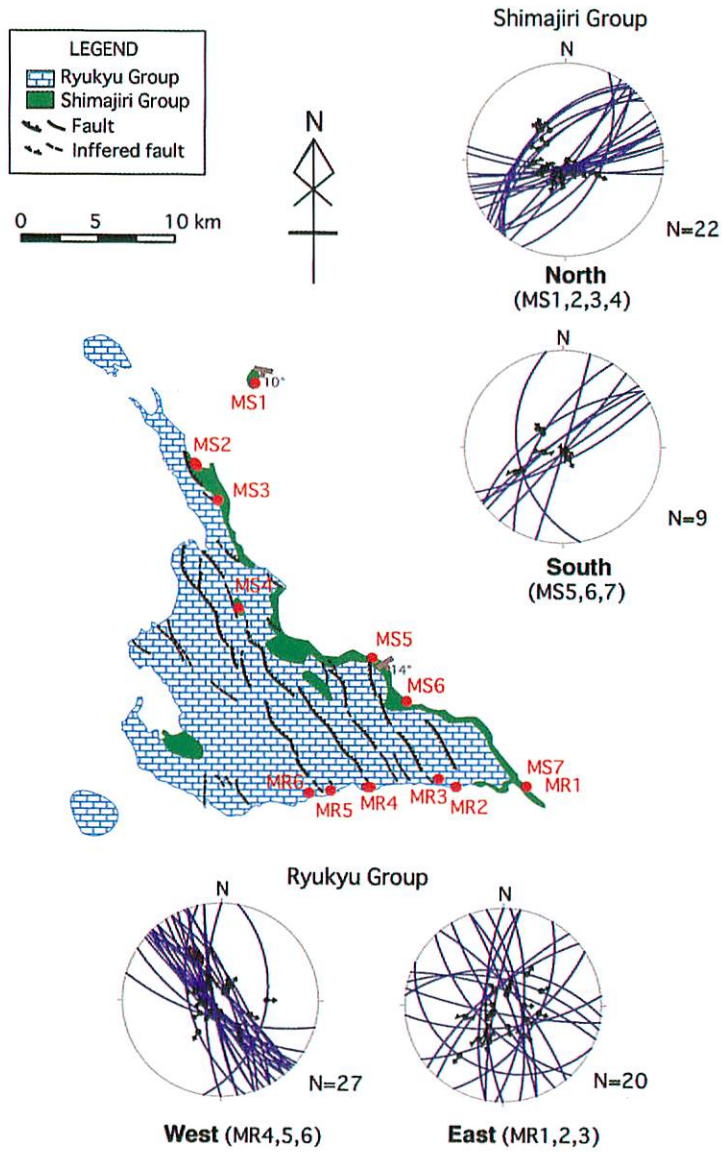

Fig. 4. Fault-slip data collected in the Miyako island. Fault-slip data are projected on lower-hemisphere, equal-area net. Arrows inside the nets indicate the sense of slip. N gives the number of slip vectors (slickenside) measured at each Group and used for computation. Geology is from Kizaki (1985) and faults are from the Research Group for Active faults in Japan (1991).

We have measured 31 fault data in the Shimajiri Group and 47 fault data in the Ryukyu Group which are grouped to four areas; North area and South area in the Shimajiri Group and West area and East area in the Ryukyu Group. Most of the faults in the Shimajiri Group and the Ryukyu Group are dip-slip normal fault or oblique-normal fault, while some are strike-slip faults. Reverse faults are not observed in the island. Strike of the fault in the Shimajiri Group is clustered to NE-SW. Strike of the faults in West area in Ryukyu Group is also clustered to NW-SE. Strike of the faults in the East area in the Ryukyu Group is radially.

4.1.2. Ishigaki island

Fig. 5 shows the fault-slip data and the site map measured in the Ishigaki island. We have measured 46 fault data in the Nosoko Formation and twelve fault data in the Ryukyu Group which are grouped into five areas; Oganzaki area, Yarabuzaki area and Tamatorizaki area in the Nosoko Formation and North area and South area in the Ryukyu Group. Faults in the Nosoko Formation are not normal faults but reverse faults. Most of the faults in the Ryukyu Group are dip-slip normal faults or oblique-normal faults while some faults are strike-slip fault. Strike of the faults in the Nosoko Formation directs radially and most of the faults in the Ryukyu Group direct to NE-SW.

4.1.3. Kohama island and Iriomote island

Fig. 6 shows the fault-slip data and the site map measured in the Kohama Island and Iriomote island. In the Kohama island, we have measured eleven fault data in the Nosoko Formation, six fault data in the Yaeyama Group and seven fault data in the Ryukyu Group. In the Iriomote island, we have measured 51 fault data in the Yaeyama Group. We have grouped the fault data in the Yaeyama Group as five areas; West area, Hoshidate area, North area, South area and Birumazaki area. Faults in the Nosoko Formation are dip-slip normal faults or oblique-normal faults. Most of the faults in the Yaeyama Group are dip-slip normal faults or oblique-normal faults, while but some faults are reverse faults. All of the faults in the Ryukyu Group are dip-slip normal faults. Although the strike of the faults in the Nosoko Formation and Yaeyama Group directs radially, faults in the Ryukyu Group are clustered to NW-SE.

4.1.3. Hateruma island

Fig. 7 shows the fault-slip data and the site map measured in Hateruma Island. We have measured 17 fault data in Ryukyu Group, which are grouped as three areas; North area, West area and South area. Faults in the Ryukyu Group are not normal fault but reverse fault. Reverse fault is prominent among the Southern Ryukyu arc. Although the strike of the faults of North area in the Ryukyu Group is clustered to NW-SE, the strike of faults observed in other area directs radially in the island.

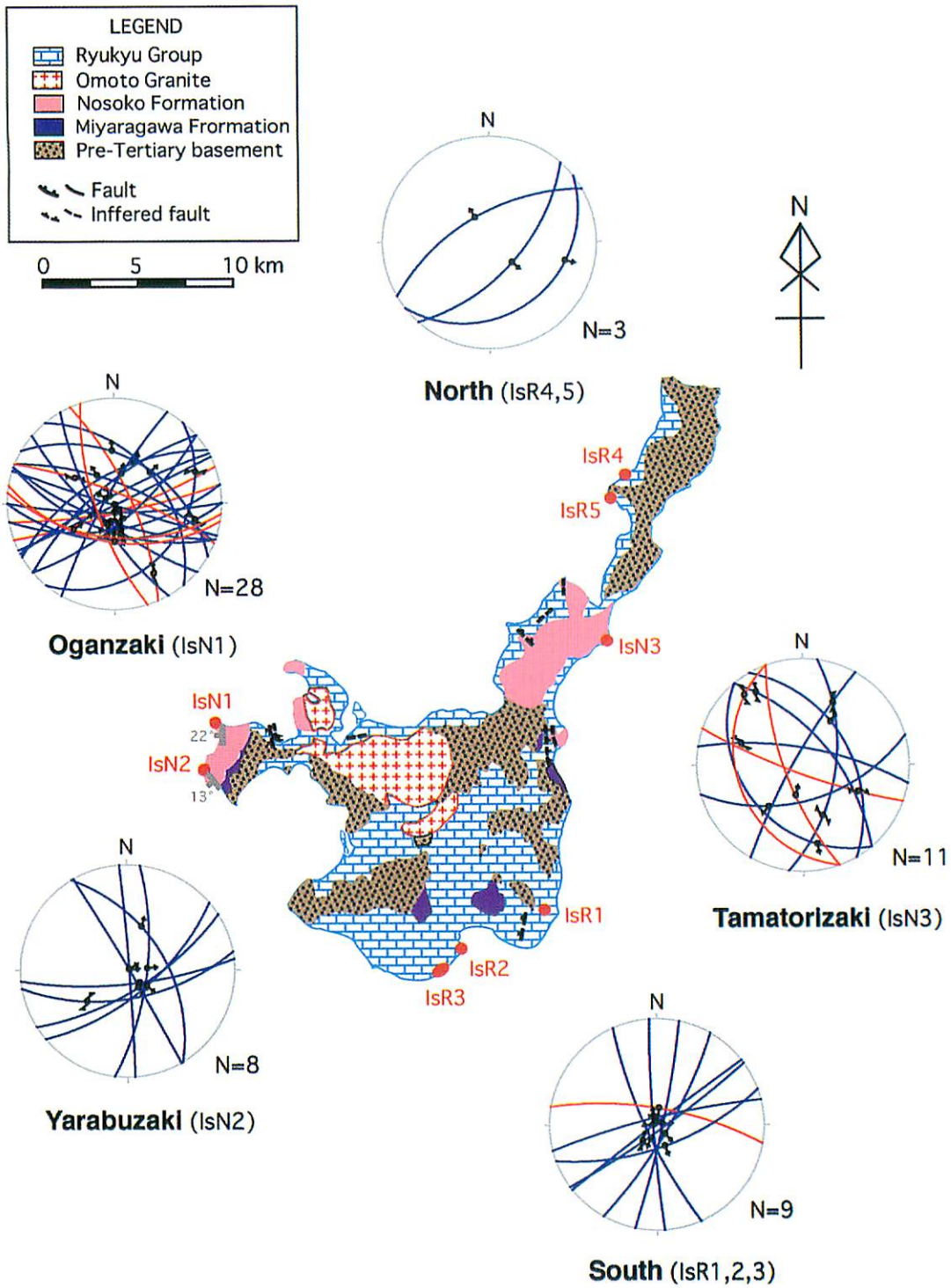

Fig. 5. Fault-slip data collected in the Ishigaki island. Explanation is same as in Fig. 4.

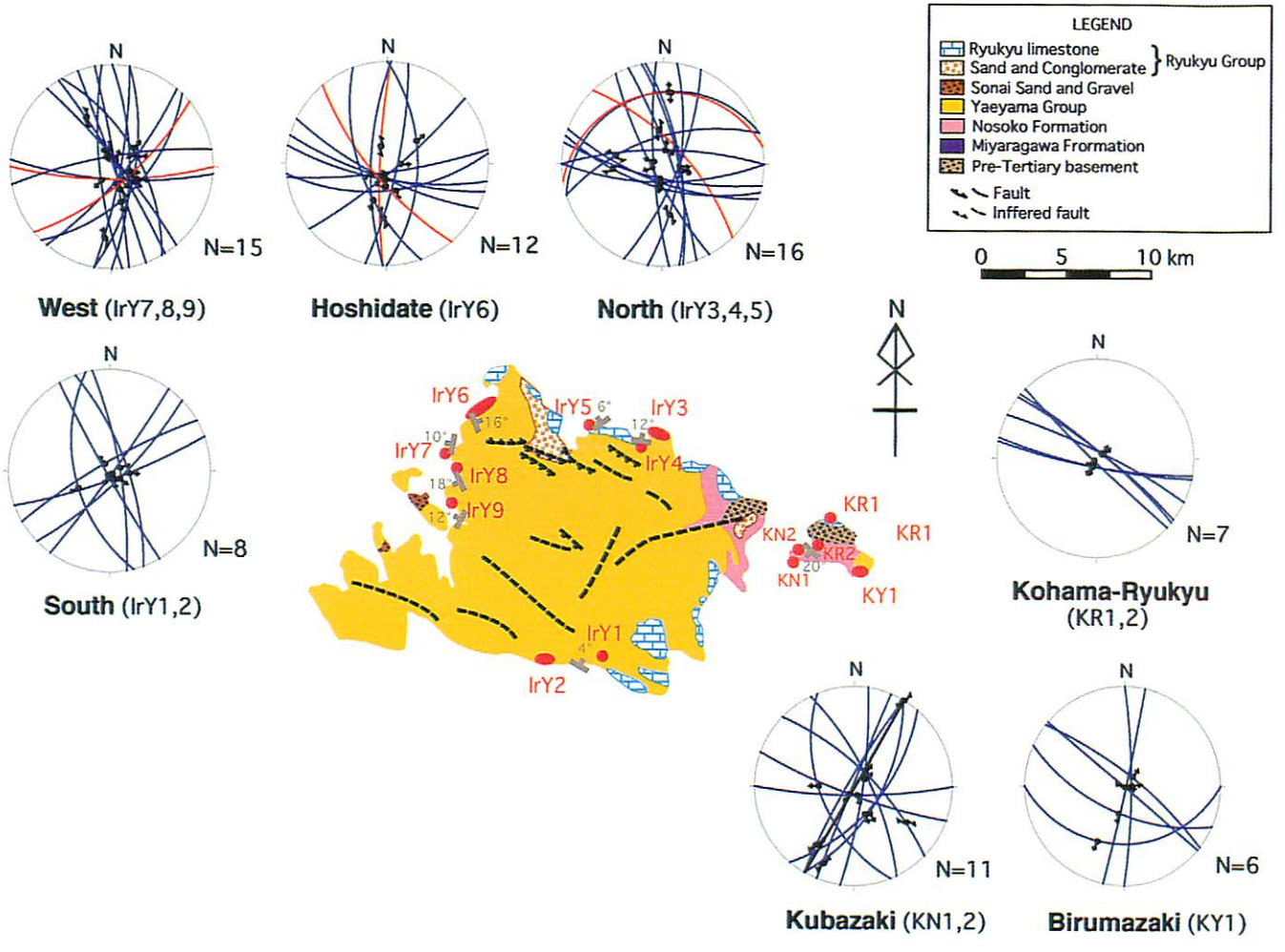

Fig. 6. Fault-slip data collected in the Kohama and Iriomote islands. Explanation is same as in Fig. 4.

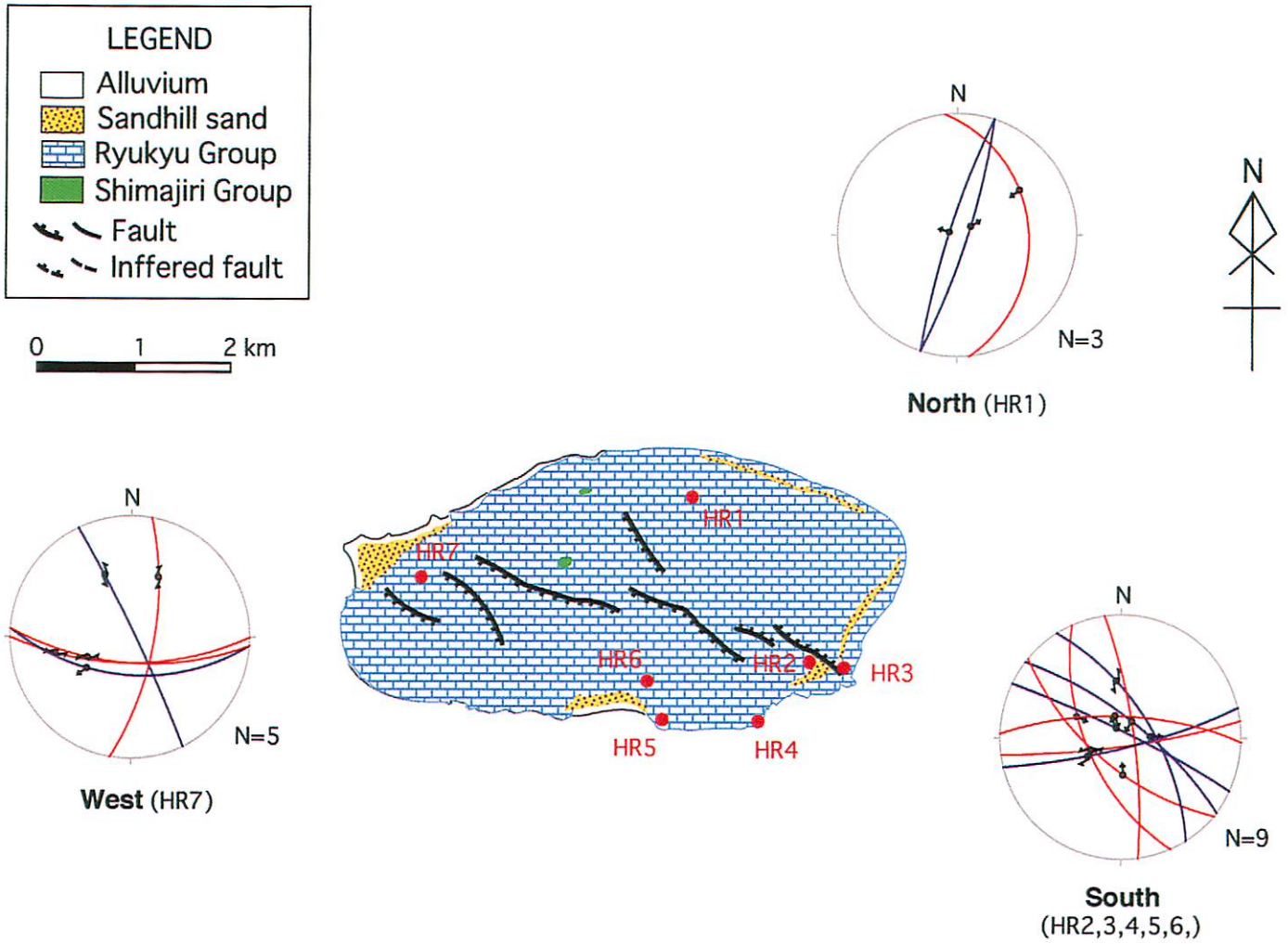

Fig. 7. Fault-slip data collected in the Hateruma island. Explanation is same as in Fig. 4.

4.1.4. Yonaguni island

Figs. 8 a and b show the fault-slip data and the site map measured in the Yonaguni Island. We have measured four fault data in the Holocene deposits, 22 fault data in the Ryukyu Group and 64 fault data in the Yaeyama Group, which are grouped these data as ten areas; East area, South area, Southwest area and West area in the Yaeyama Group, and West area, Airport area, Tyindabana area, Sonai area, Sanninudai area and Katabaruhama area in the Ryukyu Group, and Sonai area in the Holocene deposits. Most of the faults in the Yaeyama Group are dip-slip normal fault or oblique-normal fault, while

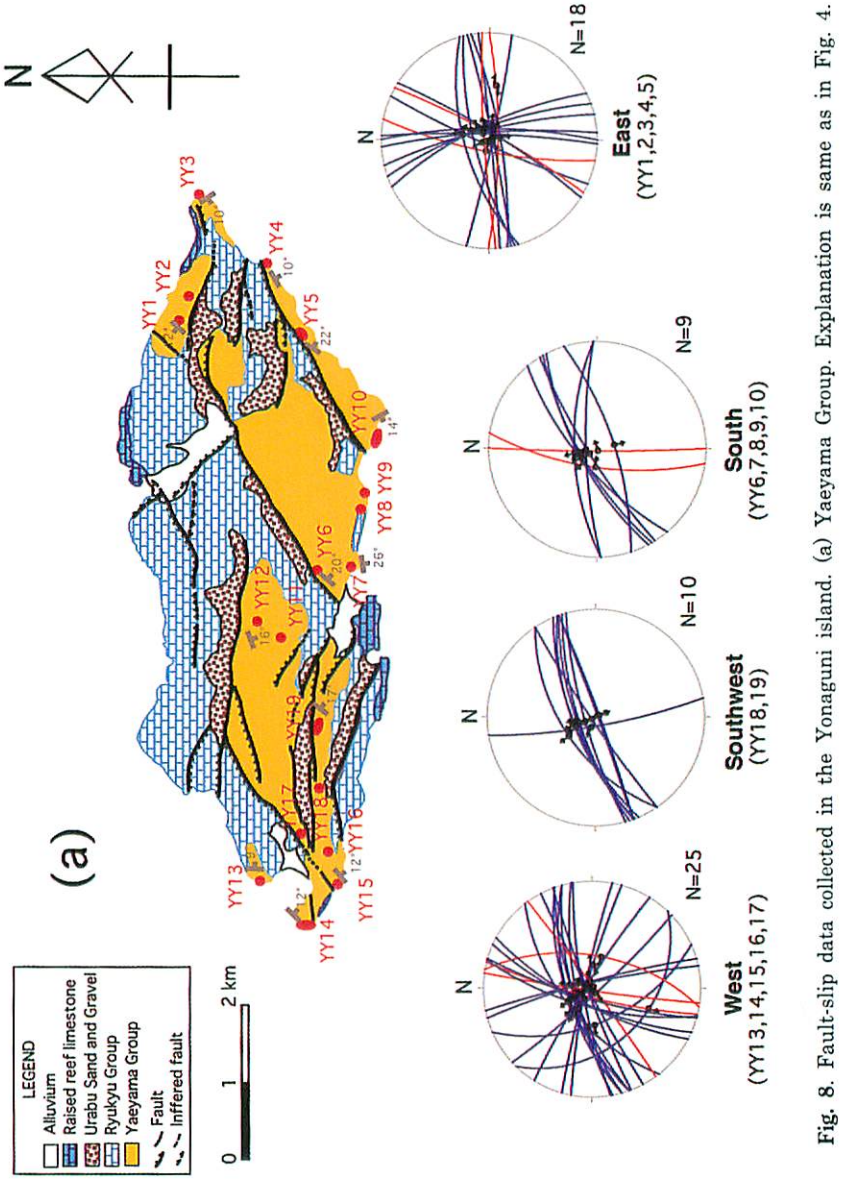

Fig. 8. Fault-slip data collected in the Yonaguni island. (a) Yaeyama Group. Explanation is same as in Fig. 4.

some faults are reverse fault. Although the strike of the fault in the Yaeyama Group in the Southwest area and South area is clustered to NE-SW like that measured by Fabbri and Fournier (1999), the strike of faults observed in other area of Yaeyama Group direct radially. Dip of most of the fault in the Yayama Group is steepness. Most of the faults in the Ryukyu Group is not normal fault but reverse fault, while some faults are oblique fault. All of the faults in the Holocene deposits are dip-slip normal faults. Strike of the faults direct to N-S to NE-SW. No reverse fault is observed in this stratum.

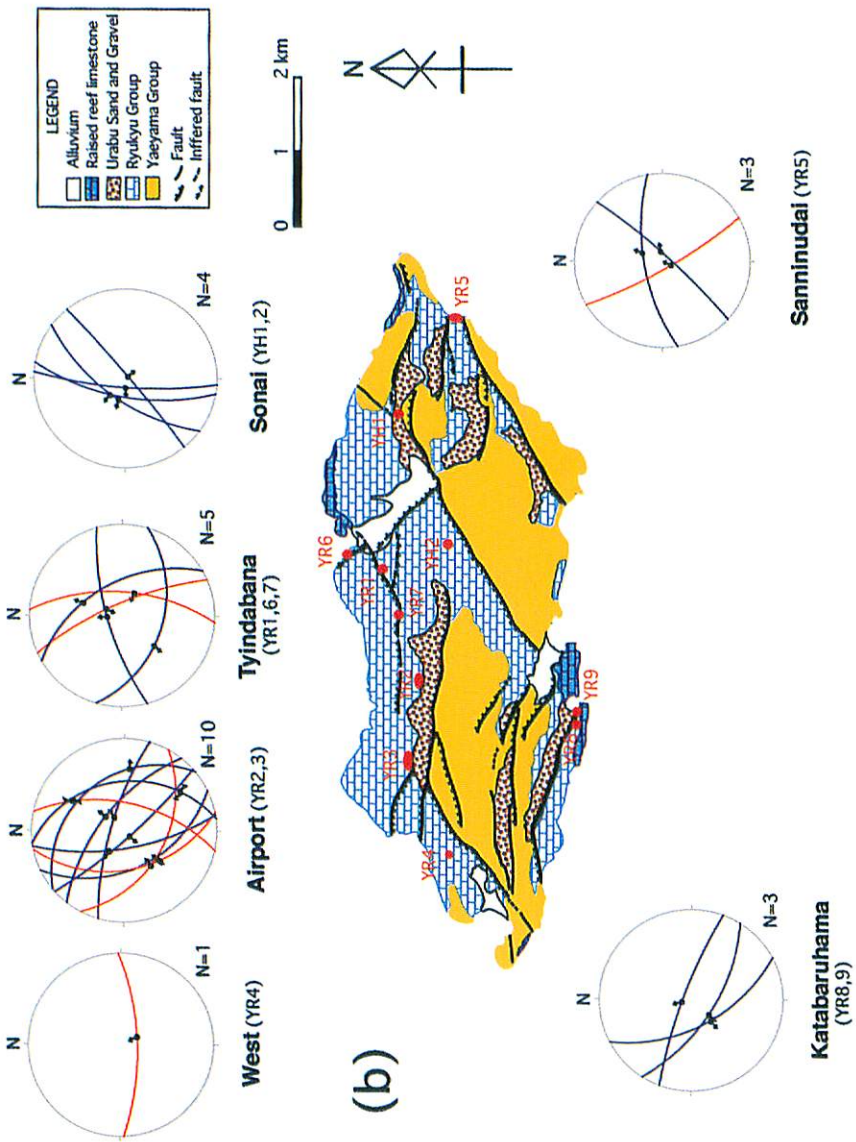

Fig. 8. (b) Ryukyu Group and Holocene deposits. Explanation is same as in Fig. 4.

4.2. Stresses detected by fault-slip analysis

We have tried to detect paleostress by the Multiple inverse method (Yamaji, 2000) and Ginkgo method (Yamaji, 2003). The Multiple inverse method with k=5 is used to most of the area in the Southern Ryukyu arc. The Ginkgo method is used to the North area of the Ryukyu Group in the Ishigaki island, Birumazaki area in the Kohama island, all area in the Hateruma island and all the area of the after Ryukyu Group in the Yonaguni island because these data is few (N<10). As the dip of strata (Nosoko Formation, Yaeyama Group, Shimajiri Group, Ryukyu Group and Holocene deposit) in the Southern Ryukyu arc is less than 26°, we do not need the tilting correction for all the data.

4.2.1. Miyako island

Fig. 9 shows the result by fault-slip analysis in the Miyako island. In MI method, the detected significant stresses are represented by clusters of dot and bar symbols in lower-hemisphere of equal-area projection. The left side figure shows the direction of σ_1 axis and the right side figure shows the direction of σ_3 axis. A dot in the right equal-area projection indicates the direction of σ_3 axis. The direction and length of the bar attached to the dot show the azimuth and plunge of the σ_1 axis of the stress state, respectively. In the left side projection, role of the dot and bar is changed with that of the right projection. Lode number is shown by rainbow colors.

Stresses A, B, C and D are identified in the Miyako island by the Multiple inverse method. The stress A is represented by the clusters of green and blue symbols, which represent a triaxial stress with vertical σ_1 axes and ENE-WSW to NE-SW trending σ_3. The stress B is represented by the clusters of yellow and green symbols, which represent a triaxial stress with NW-SE trending and 40° plunging σ_1 s1 and WNW-ESE trending and 40° plunging σ_3 axes. The stress C is represented by the clusters of blue and violet symbols, which represent a triaxial stress with NW-SE trending σ_3 and vertical σ_1 axes. The stress D is represented by the clusters of blue symbols, which represent a triaxial stress with NNE-SSW trending σ_3 and vertical σ_1 axes. We have judged that stresses A, C and D are normal faulting regime and stress B is strike-slip faulting regime under the Anderson's (1951) fault classification.

4.2.2. Ishigaki island

Fig. 10 shows the results by fault-slip analysis in the Ishigaki island. The stresses A, B, C, E, F, G, H, I, J and K were identified in the Ishigaki island by the Multiple inverse method and Ginkgo method. Stresses A, B and C are already described in the above section. The stress E is represented by the clusters of orange symbols, which represents a triaxial stress with NNE-SSW trending and 30° plunging σ_1 and NNW-SSE trending and 50° plunging σ_3 axes. The stress F is represented by the clusters of yellow and green and blue symbols, which represents a triaxial stress with E-W trending and 50° plunging σ_1

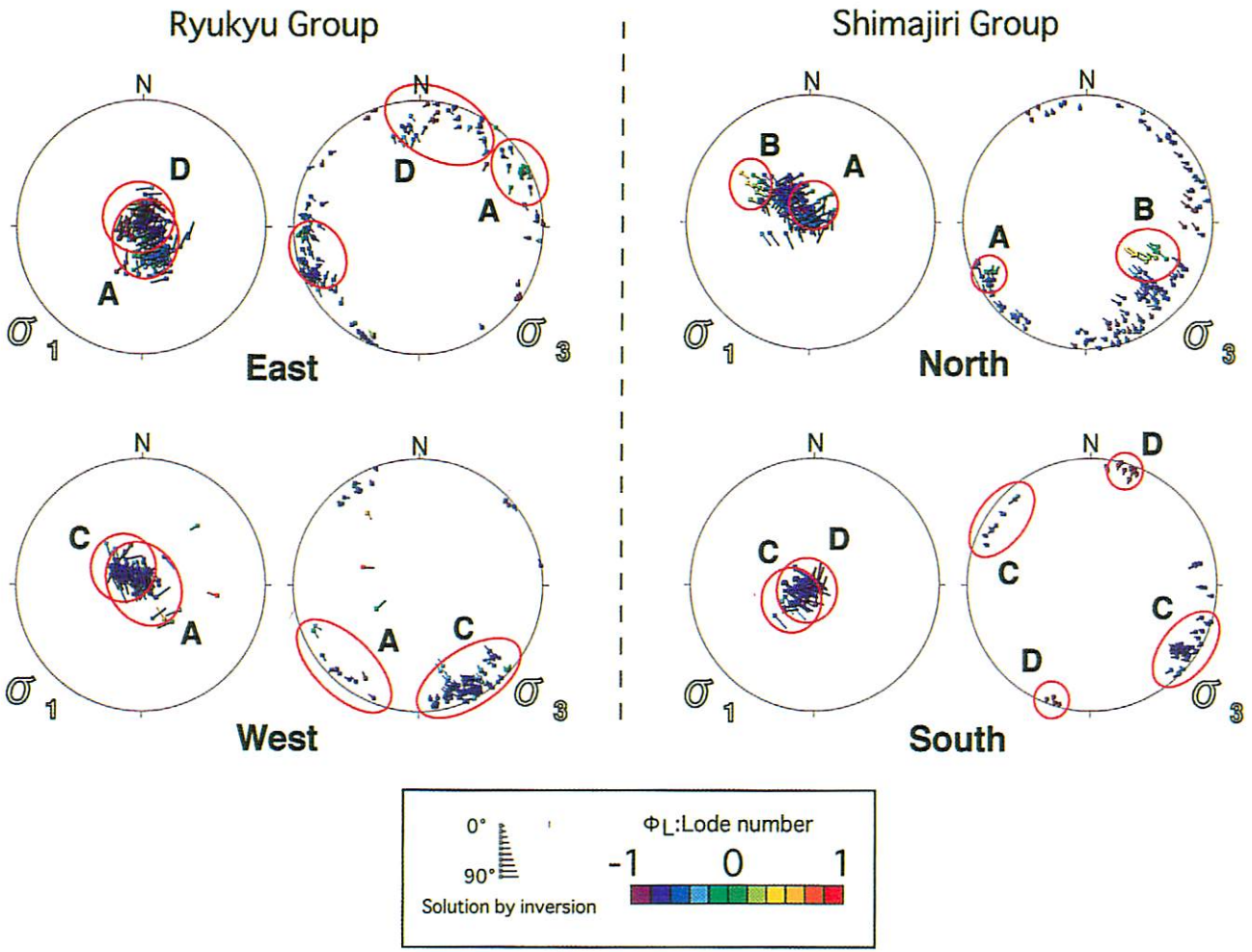

Fig. 9. Stress identified by the Multiple inverse method with k=5 from the data of the Miyako island. The clusters A, B, C and D stand out from the Shimajiri Group and Ryukyu Group.

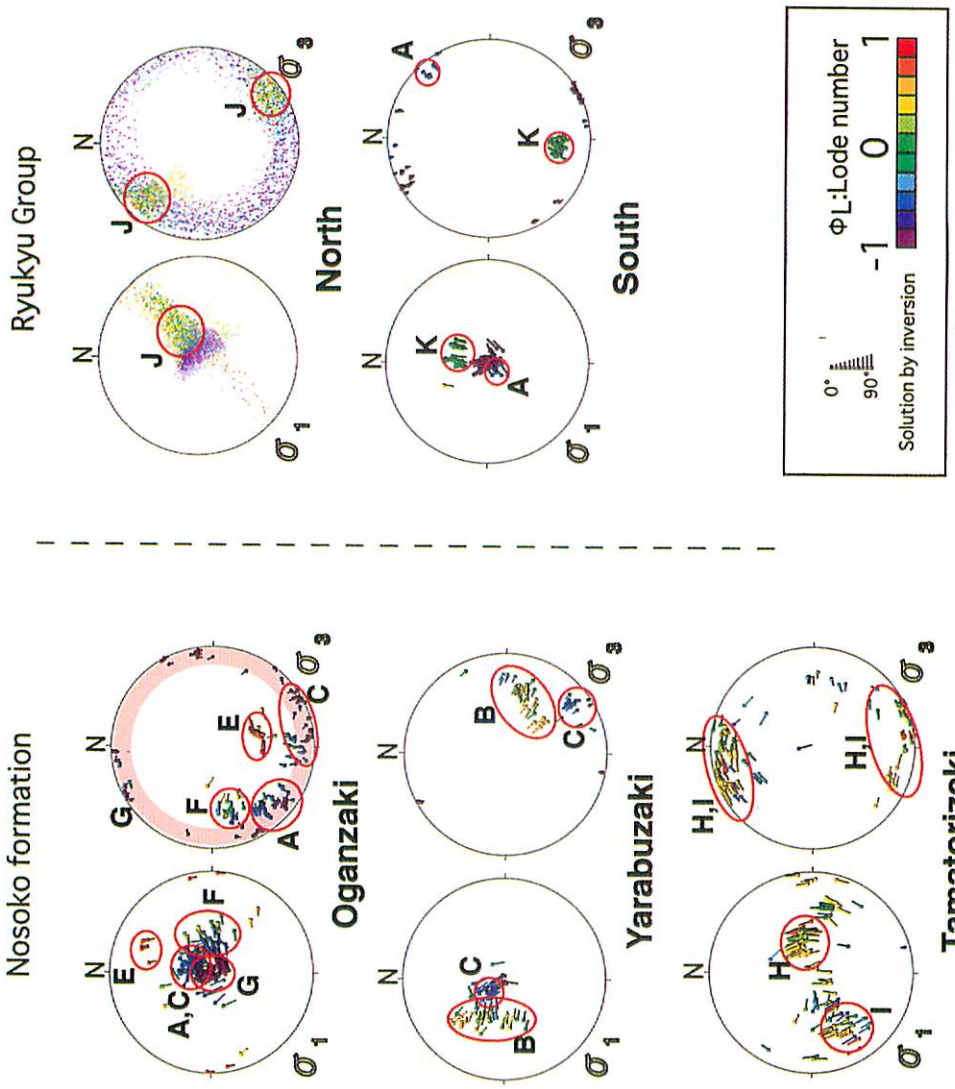

Fig. 10. Stress identified by the Multiple inverse method with k=5 and Ginkgo method from the data of the Ishigaki island. The clusters A, B, C, E, F, G, H, I, J and K stand out from the Nosoko Formation and Ryukyu Group.

and ENE-WSW trending and 30° plunging σ_3 axes. The stress G is represented by the clusters of violet symbols, which represents axial compression with vertical σ_3 axes and with σ_3 showing a great-circle girdle. The stress H is represented by the clusters of orange and yellow and green symbols, which represents a triaxial stress with ENE-SWS trending and 60° plunging σ_3 and N-S to NNW-SSE trending σ_3 axes. The stress I is represented by the clusters of orange and yellow and green symbols, which represents a triaxial stress with NE-SW trending and 25° plunging σ_1 and NNW-SSE trending σ_3 axes. The stress J is represented by the clusters of yellow and green symbols, which represents a triaxial stress with NE-SW trending and 60° plunging σ_1 and NW-SE trending σ_3 axes. The stress K is represented by the clusters of green symbols, which represents a triaxial stress with

NW-SE to WNW-ESE trending and 40° plunging σ_1 and NW-SE to WNW-ESE trending and 40° plunging σ_3 axes. We have judged that the stresses A, C, G, H, J and K belong to normal faulting regime, while the stresses B, E, F and G belong to strike-slip faulting regime under the Anderson's (1951) fault classification.

4.2.3. Kohama island and Iriomote island

Fig. 11 shows the results by fault-slip analysis in the Kohama and Iriomote island. The stresses A, C, G, L, M, N, O and P are identified in the Kohama island and Iriomote island by the Multiple inverse method and Ginkgo method. Stresses A, C and G are

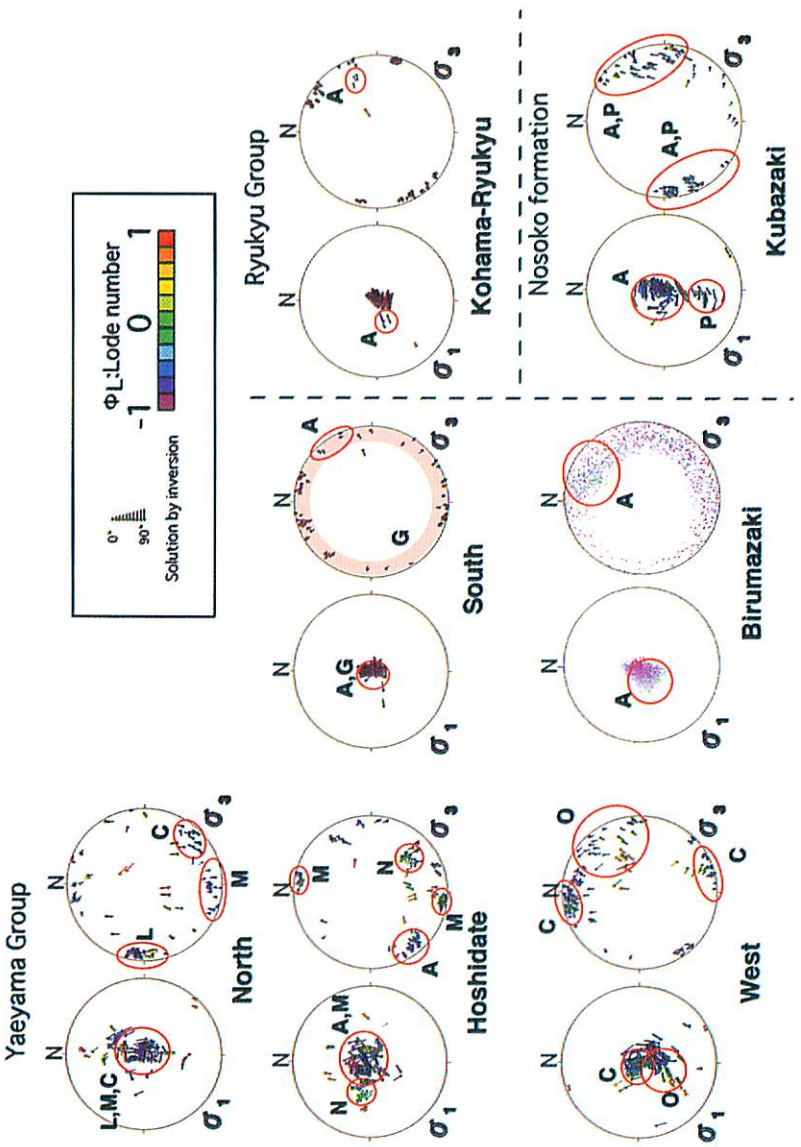

Fig. 11. Stress identified by the Multiple inverse method with k=5 and Ginkgo method from the data of the Kohama and Iriomote islands. The clusters A, C, G, L, M, N, O and P stand out from the Nosoko Formation, Yaeyama Group and Ryukyu Group.

already described in the former sections. The stress L is represented by the clusters of yellow and green and blue symbols, which represents a triaxial stress with vertical σ_1 and E-W trending σ_3 axes. The stress M is represented by the clusters of blue symbols, which represents a triaxial stress with vertical σ_1 and N-S trending σ_3 axes. The stress N is represented by the clusters of green and blue symbols, which represents a triaxial stress with E-W trending and 60° plunging σ_1 and NW-SE trending and 30° plunging σ_3 axes. The stress O is represented by the clusters of yellow and green and blue symbols, which represents a triaxial stress with NNE-SSW trending and 45° plunging σ_1 and NE-SW to ENE-WSW trending and 40° plunging σ_3 axes. The stress P is represented by the clusters of green symbols, which represents a triaxial stress with NNW-SSE trending and 30° plunging σ_1 and NE-SW to ENE-WSW trending σ_3 axes. We have judged that the stresses A, C, G, L, M and N belong to the normal faulting regime, while the stresses O and P belong to the strike-slip faulting regime under the Anderson's (1951) fault classification.

4.2.4. Hateruma island

Fig. 12 shows the results by fault-slip analysis in the Hateruma island. The stresses O, Q, R and S are identified in the Hateruma island by the Ginkgo method. Stress O is already written in the formation. The stress Q is represented by the clusters of orange and yellow and green and blue symbols, which represents a triaxial stress with ENE-SWS trending σ_1 and NNW-SSE trending and 30° plunging σ_3 axes. The stress R is represented by the clusters of red symbols, which represents axial tension with vertical σ_3 axes and σ_1 make a great-circle girdle on the base circle. The stress S is represented by the clusters of yellow symbols, which represents a triaxial stress with ENE-WSW trending and 60° plunging σ_1 and ENE-WSW trending and 40° plunging σ_3 axes. We have judged that the stress S belong to the normal faulting regime, while stresses O and Q belong to the strike-slip faulting regime and the stress R belong to the reverse faulting regime under the Anderson's (1951) fault classification.

4.2.5. Yonaguni island

4.2.5.1. Pre-Ryukyu Group

Fig. 13 a shows the results by fault-slip analysis in the pre-Ryukyu Group (Yaeyama Group) in the Yonaguni island. The stresses A, G, T, U and V are identified in the Yaeyama Group in the Yonaguni island by the Multiple inverse method. Stresses A and G are already written in the former section. The stress T is represented by the clusters of light blue symbols, which represents a triaxial stress with NW-SE trending and 70° plunging σ_1 and NW-SE trending and 25° plunging σ_3 axes. The stress U is represented by the clusters of orange and yellow and light blue symbols, which represents a triaxial stress with NE-SW to NNE-SSW trending and 30° plunging σ_1 and N-S trending and 30°

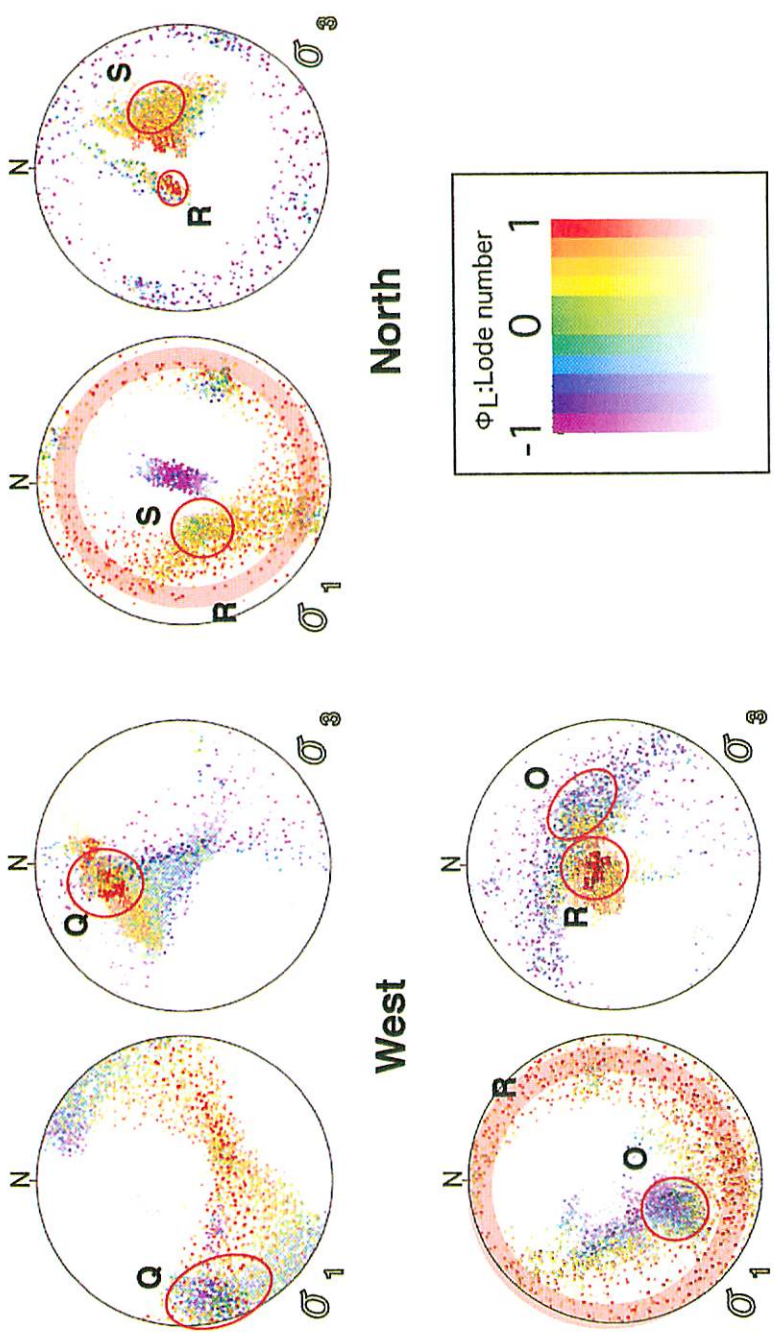

Fig. 12. Stress identified by the Ginkgo method from the data of the Hateruma island. The clusters O, Q, R and S stand out from the Ryukyu Group.

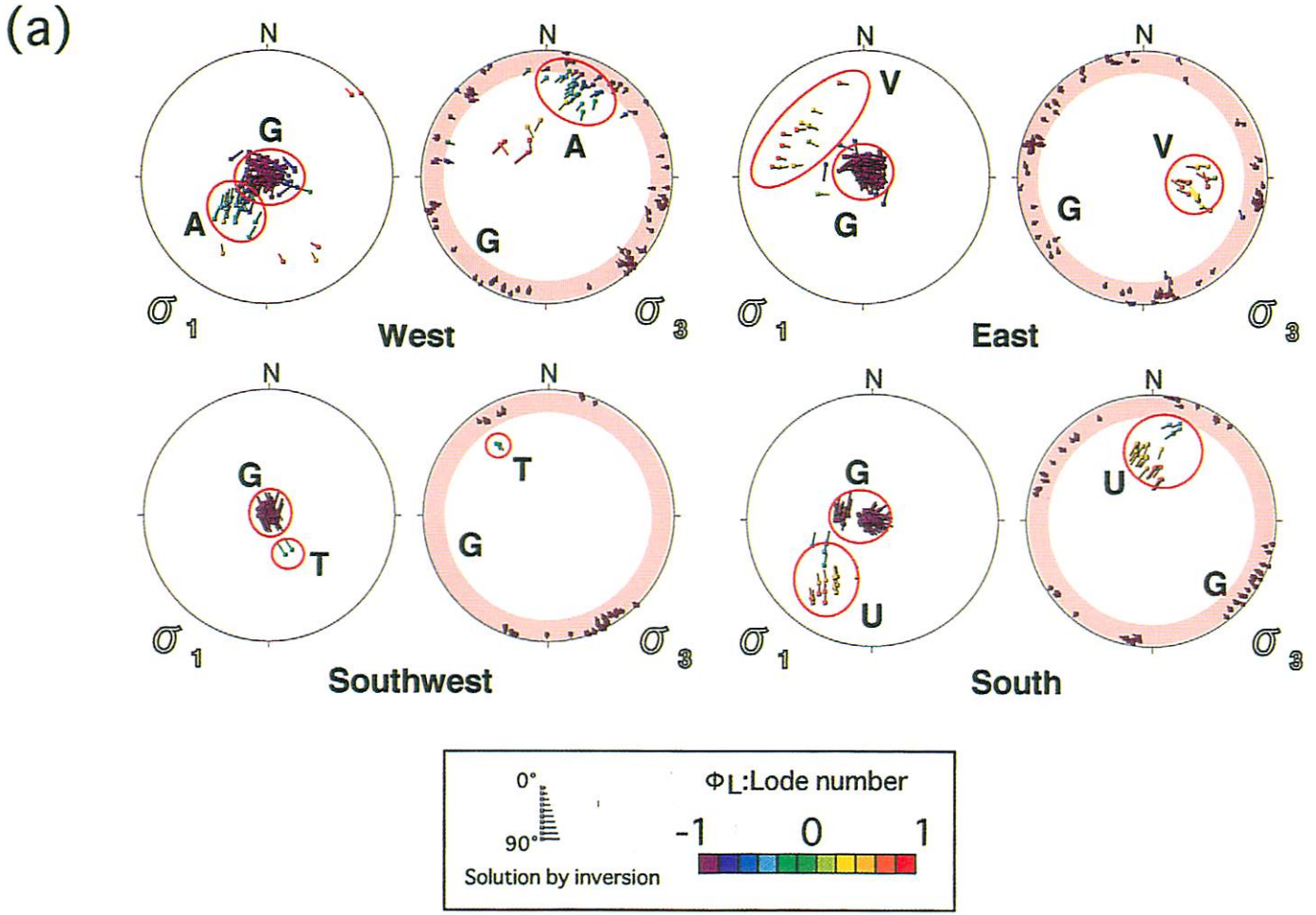

Fig. 13. Stress identified by the Multiple inverse method with $\bar{k}$=5 and Ginkgo method from the data of the Yonaguni Island. (a) The clusters A, G, T, U and V stand out from the Yaeyama Group.

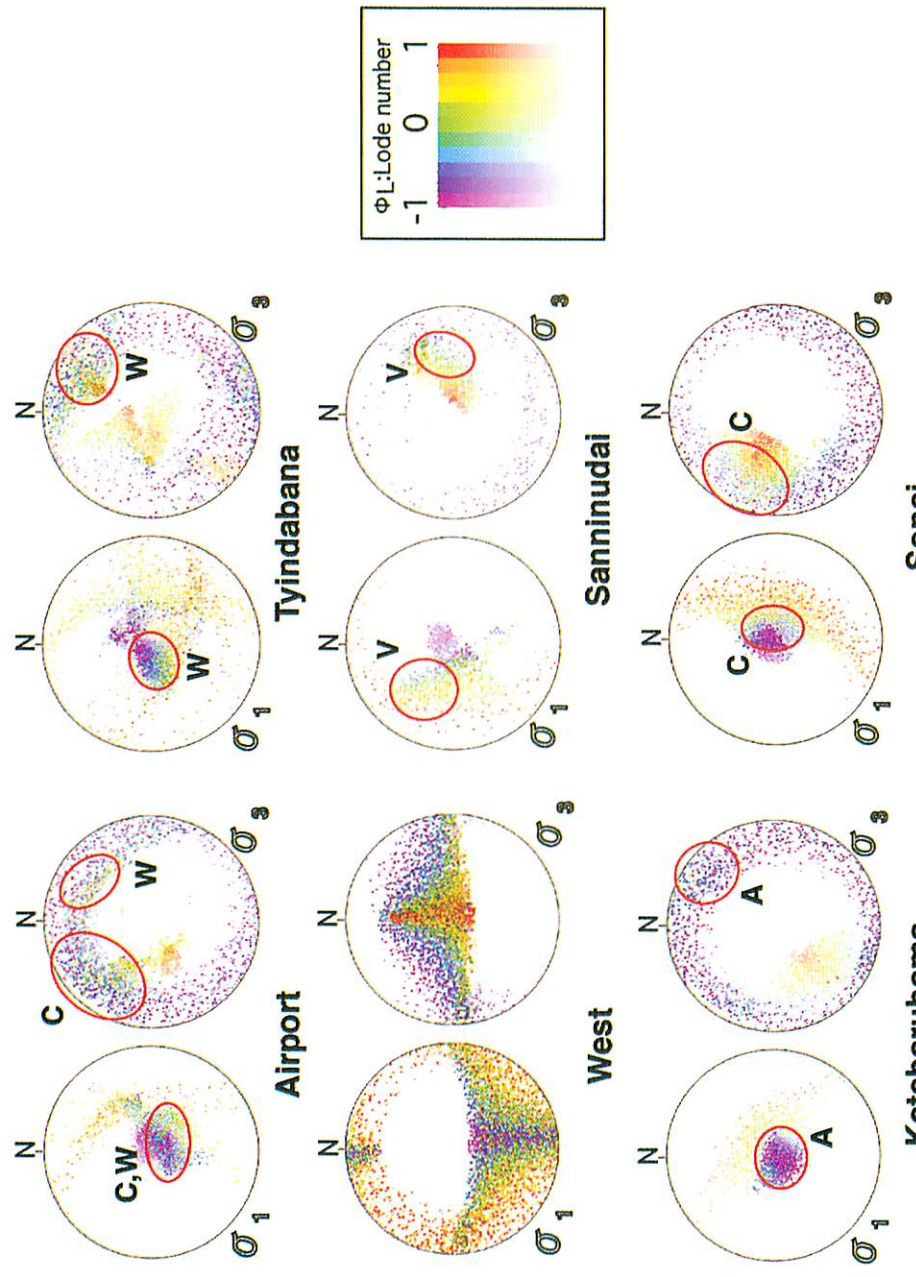

Fig. 13. (b) The clusters A, C, V and W stand out from the Ryukyu Group and Holocene deposits.

plunging σ_3 axes. The stress V is represented by the clusters of orange and yellow symbols, which represents a triaxial stress with NW-SE to WNW-ESE trending and 40° plunging σ_1 and E-W to WNW-ESE trending and 40° plunging σ_3 axes. We have judged that stress T belongs to the normal faulting regime, while the stresses U and V belong to the strike-slip faulting regime under the Anderson's (1951) fault classification.

4.2.5.2. Ryukyu Group and Holocene deosits

Fig. 13 b shows the results by the fault-slip analysis in the Ryukyu Group and Holocene deposits in the Yonaguni island. The stresses A, C, V and W are identified in the Ryukyu Group and the Holocene deposits in the Yonaguni island by the Ginkgo method. Stresses A, C and V are already described in the former sections. The stress W is represented by the clusters of green and blue symbols, which represents a triaxial stress with ENE-WSW trending and 70° plunging σ_1 and NE-SW trending and 15° plunging σ_3 axes. We have judged that the stress W belong to the normal faulting regime under the Anderson's (1951) fault classification.

4.3. Determination of age and order of detected stresses

Fig. 14 shows the synthesis of paleostress detected in the Southern Ryukyu arc. Twenty three stresses (stresses A-W) are measured from the fault-slip data in the Southern Ryukyu arc. We must decide age and order of the detected stresses. Age and order of the detected stresses are decided by (1) the stratigraphic relation of the formations which include the detected stresses, (2) the cross-cut relationship of faults and (3) the direction of stresses inferred by the earthquake focal mechanism. Fig. 15 shows the stress transition in the Southern Ryukyu arc.

4.3.1. Miyako island

Stresses A, B, C and D detected in the island are divided into three stress segments; S1 (stresses A and D), S2 (stress B) and S3 (stress C). All the stress segments S1, S2 and S3 are detected from the Shimajiri Formation. Stress segments S1 and S3 are separated from the Ryukyu Group. The lack of the stress segment S2 in the youngest Ryukyu Group suggests that the stress is older than the Group. Stress segment S3 is older than the stress segment S1 because the fault moved by the stress C cuts the fault moved by stress D. Therefore, stress transition leads to the following from old to new. The event was simultaneous with the transition from (1) strike-slip stress state composed of NW-SE compression and WNW-ESE extension (stress state M1) to (2) NW-SE extension (stress state M2), (3) NE-SW to ENE-WSW extension (stress state M3) (Fig. 15).

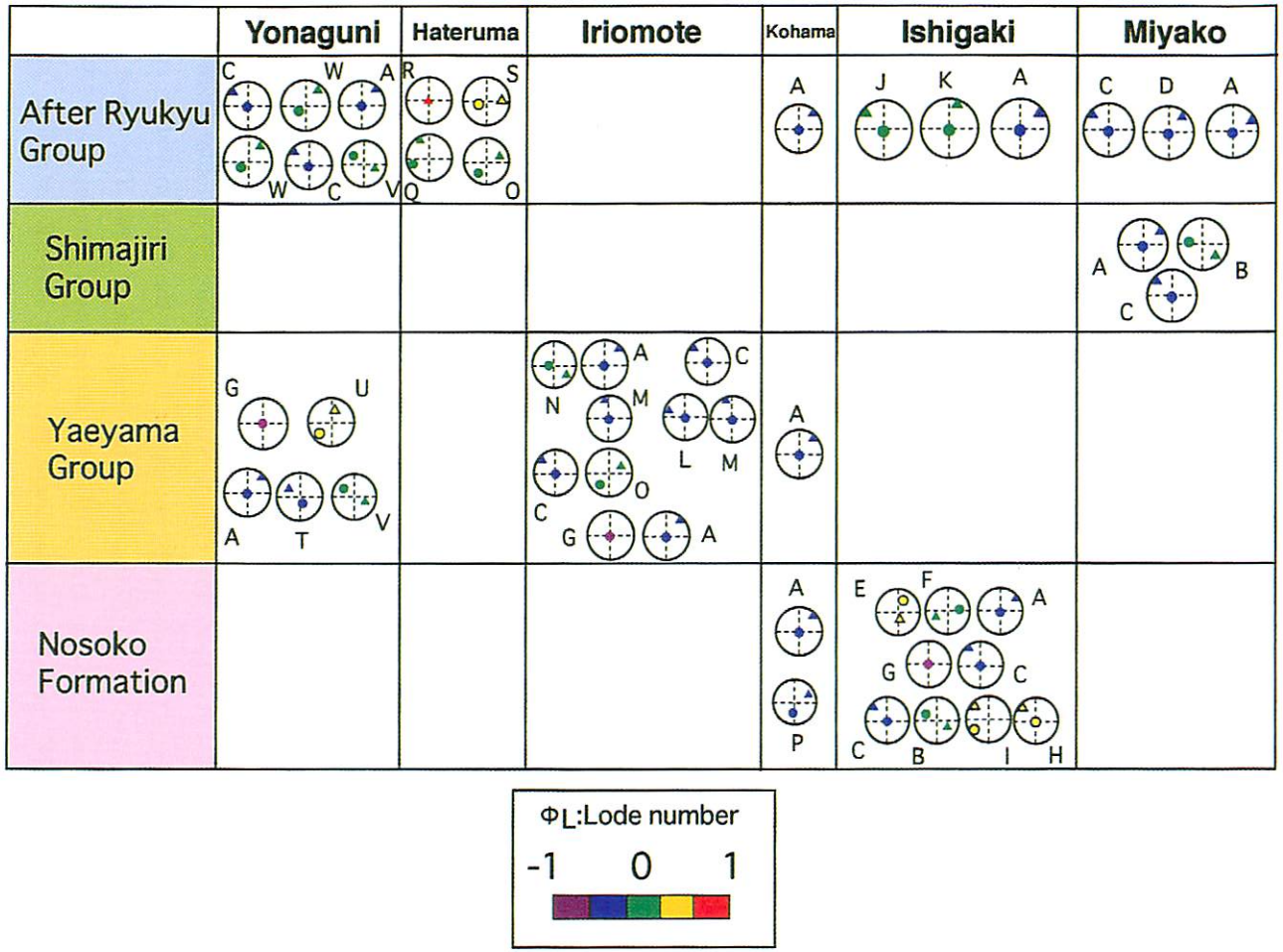

Fig. 14. Synthesis of stress pattern in the Southern Ryukyu arc by fault-slip analysis. Stress patterns are projected on lower-hemisphere, equal-area net. Circles in net indicate maximum compressional stress axis (σ_1) and triangles in the net indicate minimum compresional stress axis (σ_3). Color of the stress pattern indicates the stress ratio ($U_L=(2\sigma_2-\sigma_1-\sigma_3)\ /\ (\sigma_1-\sigma_3)$).

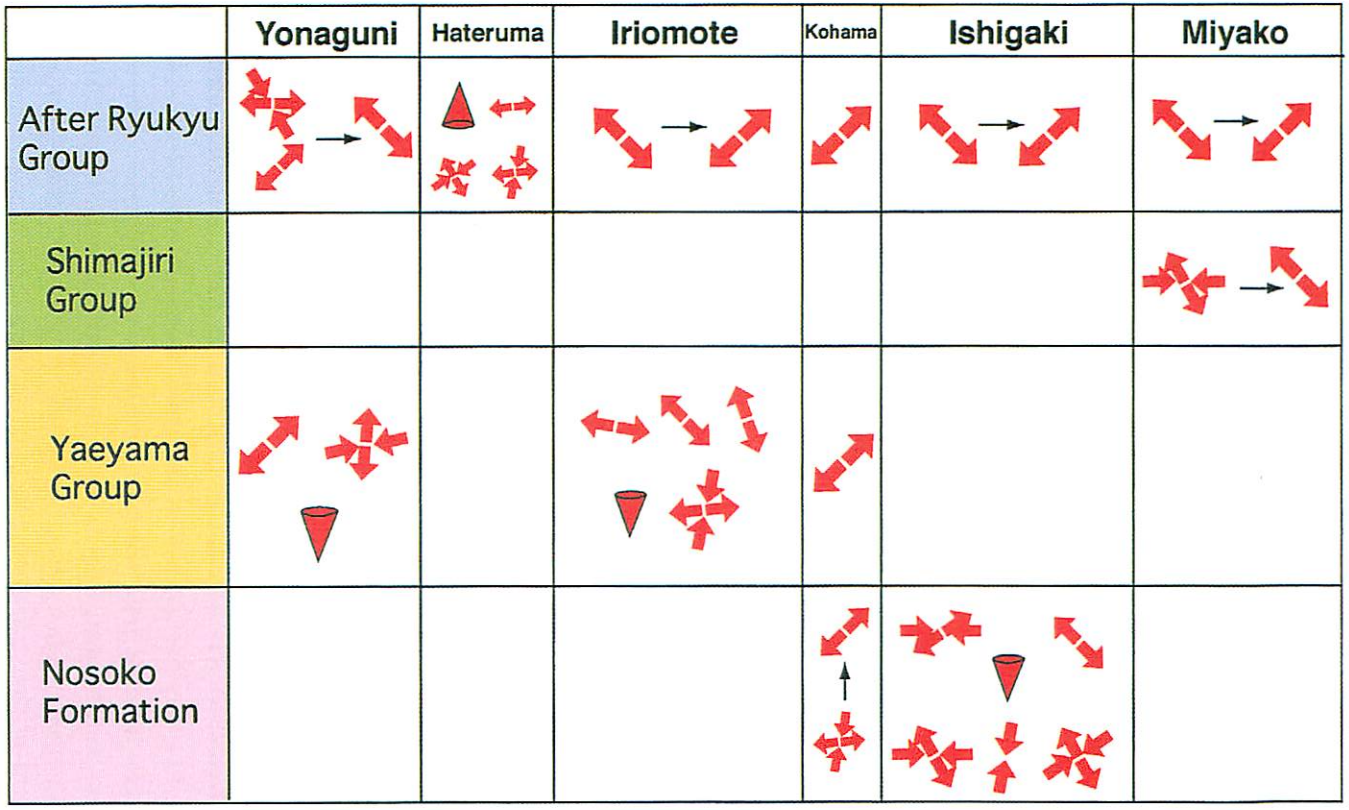

Fig. 15. Stress transition in South Ryukyu arc. Stress patterns are indicated by red arrows. Cone shows axial tension and upside-down image of cone shows axial compression.

4.3.2. Ishigaki island

Stresses A, B, C, E, F, G, H, I, J and K detected from in the island are divided into seven stress segments; S4 (stresses A and K), S5 (stress B), S6 (stresses C, H and J), S7 (stress E), S8 (stress F), S9 (stress G) and S10 (stress I). All the stress segments S4 S5, S6, S7, S8, S9 and S10 are detected from the Nosoko Formation. Stress segments S4 and S6 are separated from the Ryukyu Group. The lack of the stress segments S5, S7, S8, S9 and S10 in the youngest Ryukyu Group suggests that the stresses are older than the Group. Stress segment S6 may be older than the stress segment S4 because the present stress axis detected from the focal mechanism of earthquake occurred around Ishigaki, Kohama and Iriomote islands direct to NE-SW (Yasuda, 2002). It is difficult to decide the order of the stress segments S5, S7, S8, S9 and S10, because no cross-cut relationship of fault is observed in the island and no sedimentary beds between post-Nosoko Formation and pre-Ryukyu Group are exposed in the island. However it might be stated that the stress transition is complex before the Ryukyu Group accumulated. Therefore, stress transition is described as follows from old stress to new stress. The event was simultaneous with transition from (1) complex stress state (stress state Ih1) to (2) NW-SE extension (stress state Ih2), (3) NE-SW extension (stress state Ih3) (Fig. 15).

4.3.3. Kohama island

We do not need to group stresses because two stresses A and P are only detected. All the stresses A and P in the island are detected from the Nosoko Formation. Stress A is separated from the Yaeyama Group and the Ryukyu Group. The lack of the stress P in the youngest Yaeyama Group and Ryukyu Group suggests that the stress P is older than the Groups. Therefore, stress transition is summarized as follows from old stress to new stress. The event was simultaneous with transition from (1) Strike-slip stress state composed of NNE-SSW compression and ENE-WSW extension (stress state K1) to (2) NE-SW extension (stress state K2) (Fig. 15).

4.3.4. Iriomote island

All the stresses A, C, G, L, M, N and O are detected from the Yaeyama Group. Stresses detected from the Yaeyama Group in the island are divided into four stress segments; S11 (stress A), S12 (stresses C, L, M and N), S13 (stress G) and S14 (stress O). Stress segment S11 may be newer than the stress segments S12, 13 and 14 because the present stress axis detected from the focal mechanism of earthquake occurred around the Ishigaki, Kohama and Iriomote islands direct to NE-SW (Yasuda, 2002). Therefore, stress transition is described as follows from old to new. It is difficult to decide the order of the stress segments S12, S13 and S14 because no cross-cut relationship of faults is observed in the island. The event was simultaneous with transition from (1) complex stress state (stress state Ir1) to (2) NE extension (stress state Ir2) (Fig. 15).

4.3.5. Hateruma island

In the Hateruma island, stresses O, Q, R and S are detected from the Ryukyu Group. It is found that this area is experienced the complex stress after deposition of the Ryukyu Group because the fault in the pre and after Ryukyu Group deposits can not be observed in the island (Fig. 15).

4.3.6. Yonaguni island

Stresses A, C, G, T, U, V and W detected from in the island are divided into five stress segments; S15 (stresses A and W), S16 (stresses C and T), S17 (stress G), S18 (stress U) andS19 (stress V). All the stress segments S15, S16 S17, S18 and S19 are detected from the Yaeyama Group. Stress segments S15, S 16 and S19 are separated from the Yaeyama Group. The lack of the stress segments S17 and 18 in the youngest Ryukyu Group and Holocene deposits suggests that S17 and 18 is older than the Groups. Stress segment S15 is separated from the Ryukyu Group. The lack of the stress segments 16 and 19 in the youngest Holocene deposits suggests that the S16 and 19 is older than the Groups. It is difficult to decide the order of the stress segments S17 and S18, S16 and 19 because no cross-cut relationship of faults is observed in the island. However it might be stated that the stress transition is complex before Holocene sediments are accumulated. Therefore, stress transition is described as follows from old stress to new stress. The event was simultaneous with transition from (1) pre-Ryukyu Group complex stress state (axial compression with vertical σ_1) (stress state Y1) to (2) after Ryukyu Group complex stress state (stress state Y2), (3) NW-SE extension (stress state Y3) (Fig. 15).

4.4. Summary of fault-slip analysis

As the result of fault-slip analysis, characteristics of stress transition of the Southern Ryukyu arc are summarized as follows.

(1) Many paleostresses are existed in the Southern Ryukyu arc after the deposition of the Ryukyu Group.

(2) Stress state of the after Ryukyu Group in the western area (Yonaguni island) from 123.5° E and the area along the Ryukyu Trench (Hateruma island) is complex including strike-slip type stress state. Stress state of the after Ryukyu Group in the eastern area from 123.5° E (Miyako, Ishigaki, Kohama and Iriomote islands) is simple (from NW-SE extension to NE-SW extension).

(3) Stress state before the deposition of the Ryukyu Group in the eastern area (Iriomote and Ishigaki islands) from 123.5° E is complex including compressive and strike-slip type.

(4) Direction of latest stress in the Southern Ryukyu is are parallel to the axis of the Ryukyu arc.